European Journal of Taxonomy 870: 107–145
https://doi.org/10.5852/ejt.2023.870.2123
ISSN 2118-9773
www.europeanjournaloftaxonomy.eu
2023 · Nagy H. *et al.*

Research article

urn:lsid:zoobank.org:pub:508560B7-BD89-472A-B3FD-F48851B024C3

New insights into the *Enchytraeus albidus* complex (Annelida, Enchytraeidae), with the description of three new species from seashores in Italy and Croatia

Hajnalka NAGY[1,*], Klára DÓZSA-FARKAS[2] & Tamás FELFÖLDI[3]

[1,3]Department of Microbiology, ELTE Eötvös Loránd University, Pázmány Péter sétány 1/C, H-1117 Budapest, Hungary.
[1]Hungarian Natural History Museum, Baross utca 13, H-1088 Budapest, Hungary.
[1,2]Department of Systematic Zoology and Ecology, ELTE Eötvös Loránd University, Pázmány Péter sétány 1/C, H-1117 Budapest, Hungary.
[3]Institute of Aquatic Ecology, Centre for Ecological Research, Karolina út 29, H-1113 Budapest, Hungary.

[*]Corresponding author: nhajni6@gmail.com
[2]Email: kdozsafarkas@gmail.com
[3]Email: tamas.felfoldi@gmail.com

[1]urn:lsid:zoobank.org:author:13D87FB8-C834-4CD7-AC35-219D77009297
[2]urn:lsid:zoobank.org:author:4A08693E-3C7D-432E-8BCA-CBBDF7E36D02
[3]urn:lsid:zoobank.org:author:F0CD45C8-0140-4E52-A996-080FE186EB72

Abstract. Between 2019 and 2021, samplings were carried out from seashores in Italy and Croatia, where specimens were found morphologically similar to the species of the *Enchytraeus albidus* complex. The taxon *Enchytraeus albidus* was recently divided into a number of separate species, and the new Italian and Croatian specimens of *Enchytraeus* proved to be three additional species, all new to science, based on the results of morphological and molecular studies. In this paper, we present the description of these new species, namely *Enchytraeus adrianensis* sp. nov., *Enchytraeus andrasi* sp. nov. and *Enchytraeus andrasiformis* sp. nov., and provide additional morphological data and new reference sequences for *E. albidus* s. str., *E. krumbachi*, *E. irregularis* and further unidentified specimens that belong to the *E. albidus* group collected formerly from Hungary, Korea, Svalbard and Kerguelen Islands.

Keywords. *Enchytraeus*, Mediterranean Basin, morphological and molecular taxonomy, new enchytraeid species, seashore.

Nagy H., Dózsa-Farkas K. & Felföldi T. 2023. New insights into the *Enchytraeus albidus* complex (Annelida, Enchytraeidae), with the description of three new species from seashores in Italy and Croatia. *European Journal of Taxonomy* 870: 107–145. https://doi.org/10.5852/ejt.2023.870.2123

Introduction

Enchytraeus albidus Henle, 1837 is a well-known model organism in biological research (e.g., physiology, soil ecotoxicology) (Römbke 1989, Collado *et al.* 1999). Earlier studies (Erséus & Gustafsson 2009; Schmelz & Collado 2010) mentioned that *E. albidus* is actually a species complex. Erséus *et al.* (2019) characterized this group as follows: "Large *Enchytraeus* worms > (7.5) 10 mm; high segment number (> 40); white to yellowish; ventral chaetae 3 or more in several bundles; oesophageal appendages short, tube-like, vasa deferentia extending into segments posterior to clitellum (not always); penial bulbs surrounded by several accessory glands". Typical habitats of these species are decaying debris at seaside or compost rich in organic matter. Furthermore, Erséus *et al.* (2019) have carried out a revision of this group with extensive sampling from different countries and morphological and molecular analysis using the ITS2 region, COI and H3 genes. Based on their results, the *E. albidus* complex was resolved to contain the following species: *Enchytraeus albidus* s. str., *E. moebii* (Michaelsen, 1885), *E. albellus* Klinth, Erséus & Rota, 2019, *E.* cf. *krumbachi* (Čejka, 1913), *E. polatdemiri* Arslan & Timm, 2018 and *Enchytraeus* sp.1. Morphological differences among these species are subtle, whereas DNA-based differences are clear. The complex proved to be monophyletic. The listed species live only in seashores, except *E. albidus* s. str. and *E. polatdemiri* (Erséus *et al.* 2019). The latter was described as a new species from Lake Van, a soda lake in Turkey (Arslan *et al.* 2018). Based on COI and H3 sequence and morphological data, *E. polatdemiri* is closely related to *E. albidus* s. str., and according to the authors, *E. polatdemiri* might have evolved from a local population of *E. albidus* s. str. or from the common ancestor of these two species.

Between 2019 and 2021, samples were collected from seashores of Croatia and Italy (see Study sites). In the Croatian samples specimens of *Enchytraeus* Henle, 1837 were found, which were morphologically similar to the species of the *E. albidus* complex, but differences were also observed among them. The individuals of *Enchytraeus* found in Italy resembled *E. albidus* s. str. morphologically. The question arose whether these specimens are identical to the species highlighted and described from the *E. albidus* complex based on the results of Erséus *et al*. (2019), or whether they differ from them and represent new species. Therefore, the new specimens collected from three different coasts of the Mediterranean Basin were subjected to comparative morphological studies supplemented with molecular analyses. To obtain a more robust comparison, not only DNA sequences from the new species and reference sequences of similar species from the GenBank database were included in the molecular investigations, but some individuals of *E. albidus* s. str. from the same culture, which had been studied by Erséus *et al*. (2019). Further specimens of *Enchytraeus* were found in the Italian samples, which were identified as *Enchytraeus krumbachi* by morphological means. In addition, specimens of *Enchytraeus* from Kerguelen Islands and further individuals from Svalbard collected in 2000 (maintained in culture, frozen in 2004) and individuals from cultures of *E. irregularis* Nielsen & Christensen, 1961 from Korea and Hungary were also studied with morphological and molecular investigations. *Enchytraeus mediterraneus* Michaelsen, 1926 certainly belongs to the *E. albidus* complex (on the basis of the body size and structure of the male reproductive organ), but it clearly differs from the known species of this group in that there are no glands on the spermathecal ectal duct. It is worth noting that *E. mediterraneus* was described from Tunisia and has never been recorded again after the original description. Unfortunately, we were unable to include *E. mediterraneus* in our analyses, because we did not find individuals of *E. mediterraneus* in our samples and reference DNA sequences of *E. mediterraneus* are currently not available in the GenBank database.

As a result of our investigations, we present here the descriptions of three new species and provide additional morphological data and new reference sequences for *E. albidus* s. str., *E. krumbachi* and *E. irregularis*. We further discuss specimens of *Enchytraeus* sp.2 and *Enchytraeus* sp.3.

Material and methods

Institutional abbreviation

ELTE = Eötvös Loránd Tudományegyetem (Eötvös Loránd University), Budapest, Hungary

Abbreviations for morphological examinations and collection inventory

bp = base pair
COI = Cytochrome c Oxidase subunit I
En = letters used for holotypes in collection inventory numbers
H3 = Histone 3
ITS = Internal Transcribed Spacer
P = letters used for paratypes in collection inventory numbers
PCR = Polymerase Chain Reaction

Study sites

1. Kale Cove seashore, Adriatic Sea, Kamenjak Peninsula, Istria, Croatia, decaying *Zostera* L. debris, 44°51′13.0″ N, 13°58′50.5″ E, Júlia Török leg., 3 Apr. 2019, a culture was made from this sample and specimens were used from this culture from 1 Jul. 2019 until 14 Feb. 2020.
2. Castiglione seashore, Ligurian Sea, Italy, decaying seagrass debris, 42°45′56.0″ N, 10°52′51.0″ E, András and Kinga Dózsa-Farkas leg., 13 Dec. 2019.
3. Punta Ala Grosseto, Castiglione della Pescaia, Italy, decaying seagrass debris, 42°46′00.0″ N, 10°51′31.0″ E, András and Kinga Dózsa-Farkas leg., 24 Sep. 2020, a culture was made from this sample and specimens were used also from this culture and new samples were collected on 10 Nov. 2021.
4. Guillou Island, Kerguelen Islands, under a small clump of *Poa kerguelensis* (Hook.f.) Steud., 49°28′43″ S, 69°48′20″ E, Yves Frenot leg., 26 Mar. 2000.
5. Kongsfjorden, Svalbard, under a bird cliff ‘compost’ of bird excrements, mosses, vascular plants and nest materials, T. Birkemoe leg., 2000. From culture: 1 Oct. 2004.
6. Songcheon-dong, Jeonju-si, Jeollabuk-do, Korea, earthworm breeding box in house (food-waste), 35°50′43.0″ N, 127°08′03.1″ E, Yong Hong leg., 3 Sep. 2007. From culture: 1 Oct. 2008 and 29 Oct. 2015.
7. Érd, Hungary, sewage-sludge compost bed, 47°19′24.0″ N, 18°52′58.0″ E, Csaba Csuzdi leg., 16 Apr. 2016.

Methods of morphological examination

The enchytraeids were extracted by the wet funnel method (O’Connor 1962). From the individuals collected at study sites 1–3 and 6–7, cultures were made and specimens were used from these cultures for detailed analysis. A few specimens from the cultures (which were maintained for several years) were studied again morphologically even before the description. Enchytraeids were first investigated and measured alive, then preserved in 70% ethanol. Some specimens were stained with borax-carmine, and then passed through an ethanol (70% to absolute) dehydration series, mounted temporarily in clove oil, then permanently in Euparal between two coverslips. All important morphological characters were recorded in vivo, drawn and photographed [Axio Imager A2 microscope with differential interference contrast illumination, AxioCam MRc 5 (Zeiss) digital camera, Axiovision software]. The whole-mounted specimens were reinvestigated, measured and photographed as well. In all micrographs presented in this study, the orientation of specimens is the same: the head is either on the left side or on the top of the picture. We give the length of the first 12 segments similarly to Erséus *et al.* (2019) for comparison. Selected materials were catalogued with collection inventory numbers, letters for holotypes (‘En’) and paratypes (‘P’), and with slide numbers, and were deposited in the collection of the Department

Table 1 (continued on next page). List of specimens used for molecular taxonomic analyses with collection data and GenBank accession numbers. Sequences determined in this study appear in bold. Holotypes and paratypes of new species are indicated with H and P in parentheses. Abbreviation: n. d. = no data.

Species	Specimen ID	Locality	Habitat	Reference	ITS	COI	H3	16S rRNA
Enchytraeus adrianensis **sp. nov.**	1265 (P)	Croatia, Kale Cove	decaying *Zostera* L. debris	this study	–	**MZ750810**	**MZ816221**	–
Enchytraeus adrianensis **sp. nov.**	1266 (P)	Croatia, Kale Cove	decaying *Zostera* L. debris	this study	–	**MZ750811**	**MZ816222**	–
Enchytraeus adrianensis **sp. nov.**	1298	Croatia, Kale Cove	decaying *Zostera* debris	this study	–	**MZ750812**	**MZ816223**	**OM955219**
Enchytraeus adrianensis **sp. nov.**	1324 (P)	Croatia, Kale Cove	decaying *Zostera* L. debris	this study	–	**MZ750813**	**MZ816224**	–
Enchytraeus adrianensis **sp. nov.**	1379 (P)	Croatia, Kale Cove	decaying *Zostera* L debris	this study	–	**MZ750814**	**MZ816225**	**OM955220**
Enchytraeus adrianensis **sp. nov.**	1380 (P)	Croatia, Kale Cove	decaying *Zostera* L. debris	this study	–	**MZ750815**	**MZ816226**	**OM955221**
Enchytraeus adrianensis **sp. nov.**	1431	Croatia, Kale Cove	decaying *Zostera* L. debris	this study	–	**MZ750816**	**MZ816227**	**OM955222**
Enchytraeus adrianensis **sp. nov.**	1432	Croatia, Kale Cove	decaying *Zostera* L. debris	this study	–	**MZ750817**	**MZ816228**	–
Enchytraeus adrianensis **sp. nov.**	1463	Croatia, Kale Cove	decaying *Zostera* L. debris	this study	–	**MZ750818**	**MZ816229**	–
Enchytraeus adrianensis **sp. nov.**	1464	Croatia, Kale Cove	decaying *Zostera* L. debris	this study	–	**MZ750819**	**MZ816230**	**OM955223**
Enchytraeus andrasi **sp. nov.**	1386 (H)	Italy, Castiglione	decaying seagrass debris	this study	–	**MZ750820**	**MZ816231**	**OM955224**
Enchytraeus andrasi **sp. nov.**	1390 (P)	Italy, Castiglione	decaying seagrass debris	this study	**MZ835268**	**MZ750821**	**MZ816232**	**OM955225**
Enchytraeus andrasi **sp. nov.**	1391 (P)	Italy, Castiglione	decaying seagrass debris	this study	**MZ835269**	**MZ750822**	**MZ816233**	**OM955226**
Enchytraeus andrasiformis **sp. nov.**	1454 (P)	Italy, Punta Ala Grosseto	decaying seagrass debris	this study	**MZ835270**	**MZ750823**	**MZ816234**	**OM955227**
Enchytraeus albellus Klinth, Erséus & Rota, 2019	SM144	Greenland, Disko Island	decaying algae and sand	Erséus *et al.* 2019	–	MK266885	MK266933	–
Enchytraeus albellus Klinth, Erséus & Rota, 2019	CE6100	Sweden, Bohuslän	intertidal sand and clay	Erséus *et al.* 2019	–	MK266873	MK266932	–
Enchytraeus albellus Klinth, Erséus & Rota, 2019	CE5408	Norway, Hordaland	intertidal to shallow subtidal, sand	Erséus *et al.* 2019, Schmelz *et al.* 2019	–	MK266875	MK266927	MN248680
Enchytraeus albidus Henle, 1837	1300	Hungary, Budapest	laboratory culture	this study	–	**MZ750824**	**MZ816235**	**OM955228**
Enchytraeus albidus Henle, 1837	1301	Hungary, Budapest	laboratory culture	this study	–	**MZ750825**	**MZ816236**	–
Enchytraeus albidus Henle, 1837	1461	Hungary, Budapest	laboratory culture	this study	–	**MZ750826**	**MZ816237**	–
Enchytraeus albidus Henle, 1837	1462	Hungary, Budapest	laboratory culture	this study	–	**MZ750827**	**MZ816238**	–
Enchytraeus albidus Henle, 1837	CE23240	Norway, Troms	seashore, algal driftline	Erséus *et al.* 2019	–	MK266854	MK266922	–
Enchytraeus albidus Henle, 1837	CE16703	Greenland, Nuuk	seashore	Erséus *et al.* 2019	–	MK266865	MK266923	–
Enchytraeus albidus Henle, 1837	CE521	Sweden, Bohuslän	seashore	Erséus *et al.* 2010, Erséus *et al.* 2019	–	GU902047	MK266911	GU901785
Enchytraeus albidus Henle, 1837	CE2170	Germany, Hessen	laboratory culture	Erséus *et al.* 2019	–	MK266823	MK266912	–
Enchytraeus albidus Henle, 1837	CE11293	Portugal, Aveiro	laboratory culture	Erséus *et al.* 2019	–	MK266839	–	–
Enchytraeus albidus Henle, 1837	CE20744	Svalbard, Spitsbergen	spring	Erséus *et al.* 2019	–	MK266844	MK266921	–
Enchytraeus albidus Henle, 1837	EA–S7	Spain, A Coruna	laboratory culture	Arslan *et al.* 2018	–	MG711484	MG711505	–
Enchytraeus albidus Henle, 1837	–	Denmark, Northern Zealand	n. d.	Christensen & Glenner 2010	–	GU453370	–	–
Enchytraeus bulbosus Nielsen & Christenesen, 1963	CE798	Sweden, Västergötland	at old limestone quarry	Erséus *et al.* 2010, Erséus *et al.* 2019	–	GU902049	MK266943	GU901787
Enchytraeus christenseni Dózsa-Farkas, 1992	CE805	Sweden, Västergötland	at Lake Anten	Erséus *et al.* 2010, Erséus *et al.* 2019	–	GU902050	MK266945	GU901788

Table 1 (continued).

Species	Specimen ID	Locality	Habitat	Reference	ITS	COI	H3	16S rRNA
Enchytraeus crypticus Westheide & Graefe, 1992	CE2183	Germany, Hessen	lab culture	Erséus *et al.* 2010, Erséus *et al.* 2019	–	GU902055	MK266942	GU901789
Enchytraeus irregularis Nielsen & Christensen, 1961	262	Korea, Songcheon-dong	soil	this study	**MZ835271**	**MZ750828**	**MZ816239**	**OM955229**
Enchytraeus irregularis Nielsen & Christensen, 1961	906	Korea, Songcheon-dong	soil	this study	**MZ835272**	**MZ750829**	–	–
Enchytraeus irregularis Nielsen & Christensen, 1961	946	Hungary, Érd	soil	this study	–	**MZ750830**	**MZ816240**	**OM955230**
Enchytraeus krumbachi (Čejka, 1913)	1383	Italy, Castiglione	decaying seagrass debris	this study	**MZ835273**	**MZ750831**	**MZ816241**	**OM955231**
Enchytraeus krumbachi (Čejka, 1913)	1385	Italy, Castiglione	decaying seagrass debris	this study	**MZ835274**	**MZ750832**	**MZ816242**	**OM955232**
Enchytraeus cf. *krumbachi* (Čejka, 1913)	CE1684	Spain, Galicia	*Ulva* L compost on beach	Erséus *et al.* 2019	–	MK266870	MK266924	–
Enchytraeus cf. *krumbachi* (Čejka, 1913)	CE1689	Spain, Galicia	*Ulva* L compost on beach	Erséus *et al.* 2019	–	MK266871	MK266925	–
Enchytraeus sp.3	260	Kerguelen Islands, Ile Guillou Island	under a small clump of *Poa kerguelensis* (Hook.f.) Steud.	this study	**MZ835275**	**MZ750833**	**MZ816243**	OM955233
Enchytraeus sp.3	261	Kerguelen Islands, Ile Guillou Island	under a small clump of *Poa kerguelensis* (Hook.f.) Steud.	this study	**MZ835276**	**MZ750834**	**MZ816244**	**OM955234**
Enchytraeus sp.2	264	Svalbard, Kongsfjorden	under a bird cliff compost“	this study	**MZ835277**	**MZ750835**	**MZ816245**	**OM955235**
Enchytraeus sp.2	265	Svalbard, Kongsfjorden	under a bird cliff ‘compost’	this study	**MZ835278**	**MZ750836**	**MZ816246**	**OM955236**
Enchytraeus lacteus Nielsen & Christensen, 1961	CE813	Sweden, Västergötland	at old limestone quarry	Erséus *et al.* 2010, 2019	–	GU902052	MK266946	GU901791
Enchytraeus moebii (Michaelsen, 1885)	CE1687	Spain, Galicia	*Ulva* compost on beach	Erséus *et al.* 2019	–	MK266805	MK266904	–
Enchytraeus moebii (Michaelsen, 1885)	CE965	Sweden, Bohuslän	intertidal sand	Erséus *et al.* 2019, Schmelz *et al.* 2019	–	MK266806	MK266905	MN248679
Enchytraeus moebii (Michaelsen, 1885)	CE33458	Norway, Nordland	supralittoral, gravel	Erséus *et al.* 2019	–	MK266819	MK266901	–
Enchytraeus norvegicus Abrahamsen, 1969, year	CE804	Sweden, Västergötland	soil	Erséus *et al.* 2010, 2019	–	MK266893	MK266944	GU901793
Enchytraeus polatdemiri Arslan & Timm, 2018	CE14151	Turkey, Lake Van	zoobenthos	Erséus *et al.* 2019, Schmelz *et al.* 2019	–	MK266890	MK266939	MN248681
Enchytraeus polatdemiri Arslan & Timm, 2018	EP6	Turkey, Lake Van	zoobenthos	Arslan *et al.* 2018	–	MG711475	MG711496	–
Enchytraeus sp.1	CE4859	Greece, Skopelos	seashore, at the high–water line	Erséus *et al.* 2019	–	MK266888	MK266936	–
Enchytraeus sp.1	CE4860	Greece, Skopelos	seashore, at the high–water line	Erséus *et al.* 2019	–	MK266889	MK266938	–
Marionina vesiculata Nielsen & Christensen, 1959 (outgroup)	898	Hungary, Kőszeg	soil	this study	**MZ835279**	**MZ750837**	**MZ816247**	**OM955237**

of Systematic Zoology and Ecology, ELTE (Eötvös Loránd University, Budapest, Hungary). The last 9–12 segments from some specimens or the whole worm were used for DNA analysis.

Methods of molecular analysis

Genomic DNA was isolated from the specimens with the DNeasy Blood & Tissue Kit (Qiagen) according to the instructions given by the manufacturer. Four regions were amplified separately with PCR method: the mitochondrial cytochrome c oxidase subunit I (COI) gene, the nuclear histone 3 (H3) gene, the nuclear ribosomal ITS region and the mitochondrial 16S rRNA gene, using the primer pairs HCO2198 (5'-TAA ACT TCA GGG TGA CCA AAA AAT CA-3') and LCO1490 (5'-GGT CAA CAA ATC ATA AAG ATA TTG G-3') (Folmer *et al*. 1994), H3a- F (5'-ATG GCT CGT ACC AAG CAG ACV GC-3') and H3a-R (5'-ATA TCC TTR GGC ATR ATR GTG AC-3') (Colgan *et al*. 1998), ETTS1 (5'-TGC TTA AGT TCA GCG GGT-3') and ETTS2 (5'-TAA CAA GGT TTC CGT AGG TGA A-3') (Kane & Rollinson 1994), and Ann16SF (5'-GCG GTA TCC TGA CCG TRC WAA GGT A-3') and Ann16SR (5'-TCC TAA GCC AAC ATC GAG GTG CCA A-3') (Sjölin *et al*. 2005). If amplification failed in the case of the COI, H3 genes and ITS region, additional primer sets COI-E^{-} (5'-TAT ACT TCT GGG TGT CCG AAG AAT CA-3') (Bely & Wray 2004) and H3a-new-F (5'- TGG CTC GTA CCA AGC AGA CSG-3') with H3a-new-R (5'-ATG ATG GTG ACG CKY TTG GC-3') (AllGenetics, A Coruña) and ITS-5 (5'-GGA AGT AAA AGT CGT AAC AAG G-3') with ITS-4 (5'-TCC TCC GCT TAT TGA TAT GC-3') (White *et al*. 1990) were applied. PCR thermal profiles for COI-E^{-}, ITS-5 and ITS-4 were used as in Matamoros *et al*. (2012), and for Ann16SF and Ann16SR as in Sjölin *et al*. (2005). All other PCRs, sequencing reactions and phylogenetic analyses were conducted as described in detail previously by Dózsa-Farkas *et al*. (2015). Sanger sequencing was performed by the LGC Genomics GmbH (Berlin, Germany). In total, 12, 28 and 27 new sequences were obtained from the studied individuals of *Enchytraeus* in the case of ITS, COI and H3, respectively (Table 1). Further 19 new 16S rRNA gene sequences were generated from individuals selected for species tree reconstruction (Table 1). The lengths of the obtained gene sequences are: 568 bp for COI, 225 bp for H3 and 289 bp for 16S rRNA gene. The genes were sequenced in one direction. Sequences from members of the species of the *Enchytraeus albidus* complex (Erséus *et al*. 2019) were used for comparison. The aim of our paper is to demonstrate that our Croatian and Italian individuals of *Enchytraeus* belong to three new species, therefore one outgroup was used to root the phylogenetic trees. Sequences of *Maronina vesiculata* Nielsen & Christensen, 1959 were used as outgroup, because members of the *Marionina* Michaelsen, 1890 genus appeared relatively close to *Enchytraeus* on the phylogenetic tree in Erséus *et al*. (2010) and sequences of *Maronina vesiculata* were determined from all studied genes. Unfortunately, we failed to amplify the ITS region from many specimens of *Enchytraeus*, which was probably due to the improper hybridization of PCR primer sequences to the extracted genomic DNA because the ITS sequence chromatograms contained mixed positions in many cases. Another possible reason can be that ITS is a fast-evolving nuclear region and it can often show heterozygosity. Besides, the variation can involve length differences, thus even more mixed positions will appear on the chromatograms. An ITS tree was not estimated due to the above mentioned reasons and absence of whole ITS sequences (containing ITS1, 5.8S rDNA and ITS2) from species of the *E. albidus* group in GenBank. The construction of maximum likelihood gene trees, including the search for the best-fit model was carried out with the MEGA 7 software (Kumar *et al*. 2016). According to the results of model test the following nucleotide substitution models were applied in the construction of gene trees for COI and H3 genes: COI gene, GTR+G+I; H3 gene, K2+G. One species tree was created from COI, H3 and 16S rRNA genes using the BEAST ver. 2.3.2 package (Bouckaert *et al.* 2014). A total of 28 specimens from 16 species (15 different species of *Enchytraeus* and one outgroup species) were included in the analysis. Alignments of the three genes were imported into BEAUti ver. 2.3.2 (Bouckaert *et al.* 2014), where the *BEAST (STARBEAST) option was selected. The *BEAST module allows species tree estimation under the multispecies coalescence model (Heled & Drummond 2010). The applied nucleotide substitution models were the follows: GTR+G+I for COI, TN93+G for H3 and GTR+G for the 16S rRNA gene. Empirical

base frequencies were used for all genes. Clock models were separate strict clocks, clock rate of COI was set to 1 and estimated for H3 and 16S rRNA gene. The Yule process speciation prior was used and the linear and constant root was selected for species tree population size model. Ploidy type was changed to mitochondrial for 16S and COI genes. For all genes, normally distributed priors were used for the clock rates (clock.rate). Exponential distribution with mean 1 was selected for species population mean and mean growth rate priors. Default settings were used for all other priors. All these adjustments were based on those given by Erséus *et al*. (2019). From these settings, an XML input file was created in BEAUti ver. 2.3.2 and this XML file was imported into BEAST ver. 2.3.2 (Bouckaert *et al.* 2014). The analysis ran for 100 million generations, sampling every 10 000 generations. Tracer ver. 1.7.2 (Rambaut *et al*. 2018) was used to examine the resulting log-file and determine burn-in. The first 5% of trees was discarded as burn-in, and the remaining trees were summarized with TreeAnnotator ver. 2.3.2 (Bouckaert *et al.* 2014) using the maximum clade credibility tree option. The species tree was drawn in FigTree ver. 1.4.4 (tree.bio.ed.ac.uk/software/figtree/). Gene trees and the species tree were edited with CorelDRAW 2021 (www.coreldraw.com) and Inkscape ver. 0.92.4 (https://inkscape.org). Besides the phylogenetic tree estimations, pairwise genetic distances between COI and between H3 sequences of the new species and members of the *E. albidus* complex were calculated in MEGA 7.0 using the p-distance method. Gaps and missing data were excluded using pairwise deletions. These settings are based on Martinsson & Erséus (2018). Sequences obtained in this study were deposited in GenBank under the following accession codes: MZ835268-MZ835279 (ITS), MZ750810-MZ750837 (COI), MZ816221-MZ816247 (H3), OM955219-OM955237 (16S rRNA gene).

Results

Taxonomy

Class Clitellata Michaelsen, 1919
Order Enchytraeida Kasprzak, 1984
Family Enchytraeidae d'Udekem, 1855
Genus *Enchytraeus* Henle, 1837

Enchytraeus adrianensis sp. nov.
urn:lsid:zoobank.org:act:B49B8279-3D90-408F-B45C-BF89ACFC3C2B
Figs 1A, 2–3, Tables 1–2

Diagnosis

(1) Body length 14–30 mm (in vivo), segment number 51–84; (2) chaetae maximum 4 per bundle, straight with ental hook; (3) clitellum in XII–XIII, hyalocytes and granulocytes in dense transverse rows dorsally and laterally (or in a reticulate pattern), mostly only granulocytes between the male pores; (4) epidermal gland cells in 3–4 rows / segments, often brownish; (5) four pairs of nephridia preclitellarly; (6) pharyngeal glands widely or slightly connected dorsally and with ventral lobes; (7) dorsal blood vessel origin from XIV–XV, blood colourless; (8) sperm funnel cylindrical, 350–690 µm long, 2–4 × as long as wide in vivo; (9) vasa deferentia tripartite, extending into XV–XIX, the slender part ciliated, the thickened middle section not ciliated; (10) male glands multiple: one large rounded primary bulb (60–125 µm long and 50–95 µm wide), and 6–9 smaller secondary glands, ventral recess between the male copulatory organs absent; (11) spermathecal ectal duct (90–160 µm long in vivo) covered with gland cells, ampulla oval or spherical (70–115 µm wide) with wide wall and without diverticula, connecting with oesophagus; (12) 2–7 mature eggs present at a time.

Etymology

Named after the Adriatic Sea where it was found.

Material examined

Holotype

CROATIA • Istria, Kamenjak Peninsula, Adriatic Sea, Kale Cove, seashore, decaying *Zostera* debris; 44°51′13.0″ N, 13°58′50.5″ E; 3 Apr. 2019; Júlia Török leg., from culture: 15.10.2019, En.2. slide 2842; ELTE.

Paratypes (21 specs)

CROATIA • 1 spec.; same collection data as for holotype; slide 2841a,b; P.143.1; ELTE • 1 spec., last 19 segments, 3 mm used for DNA analysis (No. 1265, ID number); same collection data as for holotype; slide 2717; P.143.2; ELTE • 1 spec.; same collection data as for holotype; slide 2748; P.143.3; ELTE • 1 spec., last 18 segments, 2.3 mm used for DNA analysis (No. 1324, ID number); same collection data as for holotype; slide 2750; P.143.4; ELTE • 1 spec., last 15 segments, 3 mm used for DNA analysis (No. 1266, ID number); same collection data as for holotype; slide 2751; P.143.5; ELTE • 1 spec.; same collection data as for holotype; 2760; P.143.6; ELTE • 1 spec.; same collection data as for holotype; slide 2822a–c; P.143.7; ELTE • 1 spec.; same collection data as for holotype; slide 2827a,b; P.143.8; ELTE • 1 spec.; same collection data as for holotype; slide 2850; P.143.9; ELTE • 1 spec.; same collection data as for holotype; slide 2851a,b; P.143.10; ELTE • 1 spec.; same collection data as for holotype; slide

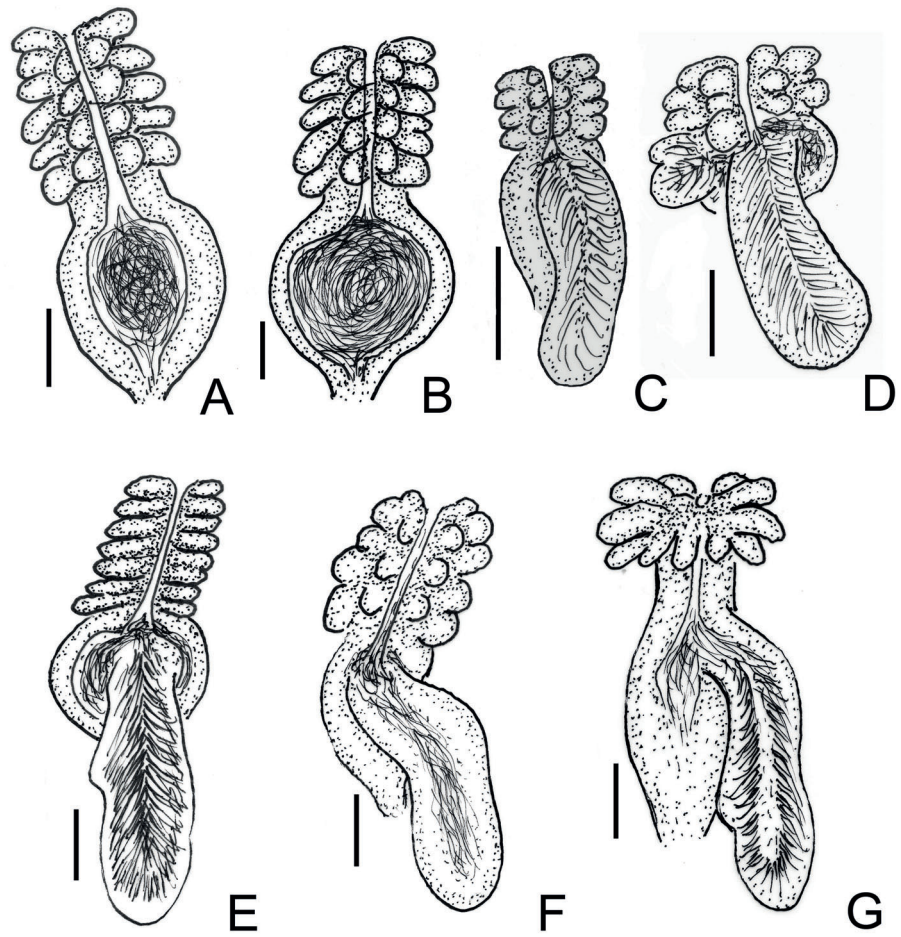

Fig. 1. Schematic drawing of spermathecae of the specimens studied. **A**. *Enchytraeus adrianensis* sp. nov. **B**. *E. krumbachi* (Čejka, 1913). **C–D**. *E. andrasi* sp. nov. **E**. *E. andrasiformis* sp. nov. **F**. *E. albidus* Henle, 1837. **G**. *E. irregularis* Nielsen & Christensen, 1961.

2852a,b; P.143.11; ELTE • 1 spec.; same collection data as for holotype; slide 2853; P.143.12; ELTE • 1 spec. [last 16 segments, 2.2 mm used for DNA analysis (No. 1379, ID number)]; same collection data as for holotype; slide 2854; P.143.13; ELTE • 1 spec.; same collection data as for holotype; slide 2855; P.143.14; ELTE • 1 spec., last 22 segments, 2.7 mm used for DNA analysis (No. 1380, ID number); same collection data as for holotype; slide 2856; P.143.15; ELTE • 1 spec.; same collection data as for holotype; slide 2857; P.143.16; ELTE • 1 spec.; same collection data as for holotype; slide 2858; P.143.17; ELTE •1 spec.; same collection data as for holotype; slide 2859; P.143.18; ELTE • 1 spec.; same collection data as for holotype; slide 2861; P.143.19; ELTE • 1 spec.; same collection data as for holotype; slide 3010; P.143.20; ELTE • 1 spec.; same collection data as for holotype; slide 3011; P.143.21; ELTE.

Other material

CROATIA • 15 specs; same collection data as for holotype; ELTE • 3 specs (only for DNA analysis); same collection data as for holotype; ELTE.

Description

Measurements. Large specimens. Holotype 22.8 mm long, 570 μm wide at VIII and 770 μm at clitellum, fixed, segment number 60. Body length of paratypes 14–30 mm, width 450–780 μm at VIII and 550–1000 μm at clitellum, in vivo. Length of fixed specimens 7.7–24.9 mm (in one specimen 28.2 mm, width 410–730 μm at VIII and 490–950 μm at clitellum). Length of the first 12 segments 2.2–4.8 mm, after fixation. Segment number 51–84 (N = 34).

Chaetae. Chaetal formula according to Schmelz & Collado (2010): 2,3–2,3:3,4–2,3. Chaetae straight with ental hook, about equal in size within bundle, 72–112 μm × 5–7.5 μm preclitellarly and 70–100 μm × 5–7.5 μm posteriorly. In ventral preclitellar bundles of some specimens 3 chaetae, and only one or two bundles with 4 chaetae, in other specimens 4 chaetae in most of all other bundles. Often 2–3 surplus chaetae near the bundles (Fig. 2B). Chaetae in XII absent ventrally, but 2–3 per bundle present laterally.

Head pore. At 0/I.

Epidermal glands. Often brown, arranged in 3–4 rows per segment.

Clitellum. Girdle-shaped, in XII–XIII, hyalocytes and granulocytes in dense transverse rows dorsally and laterally (Fig. 2C), but in well-developed sexual condition gland cells in reticulate pattern (Fig. 2D). Mostly only granulocytes between male pores (Fig. 2E–F).

Brain. About 1.3–1.8 × as long as wide, rounded posteriorly, sides slightly merging anteriad often with 2 small aggregations of refractile globules (Fig. 2A).

Oesophageal appendages. Pair of blind-ending tubes in III/IV, with common root inserting dorsally behind pharyngeal pad. Mostly all primary pharyngeal glands widely or slightly connected dorsally with ventral lobes (Fig. 2H). In some specimens first pair separate (Fig. 2G). Ventral lobes of third pair largest.

Dorsal blood vessel. From XIV–XV, blood colourless. Anterior bifurcation near prostomium.

Nephridia. Four pairs of preclitellar nephridia from 6/7–9/10, anteseptale funnel only, postseptale bulged, efferent duct short, origin postero-ventrally.

Coelomocytes. Oval or narrowed at one end, texture granulated, about 24–40 μm long, in vivo (Fig. 2I–J) [15–30 μm, fixed (Fig. 2K)]. In addition, many shining, hyaline, round or tetragonal corpuscles

[diameter (10–19 µm)] also present (Fig. 2J), which at lower magnification shine like grains of sand. In young specimens corpuscles always fewer. Note, corpuscles not visible after fixation.

Subneural glands. Absent.

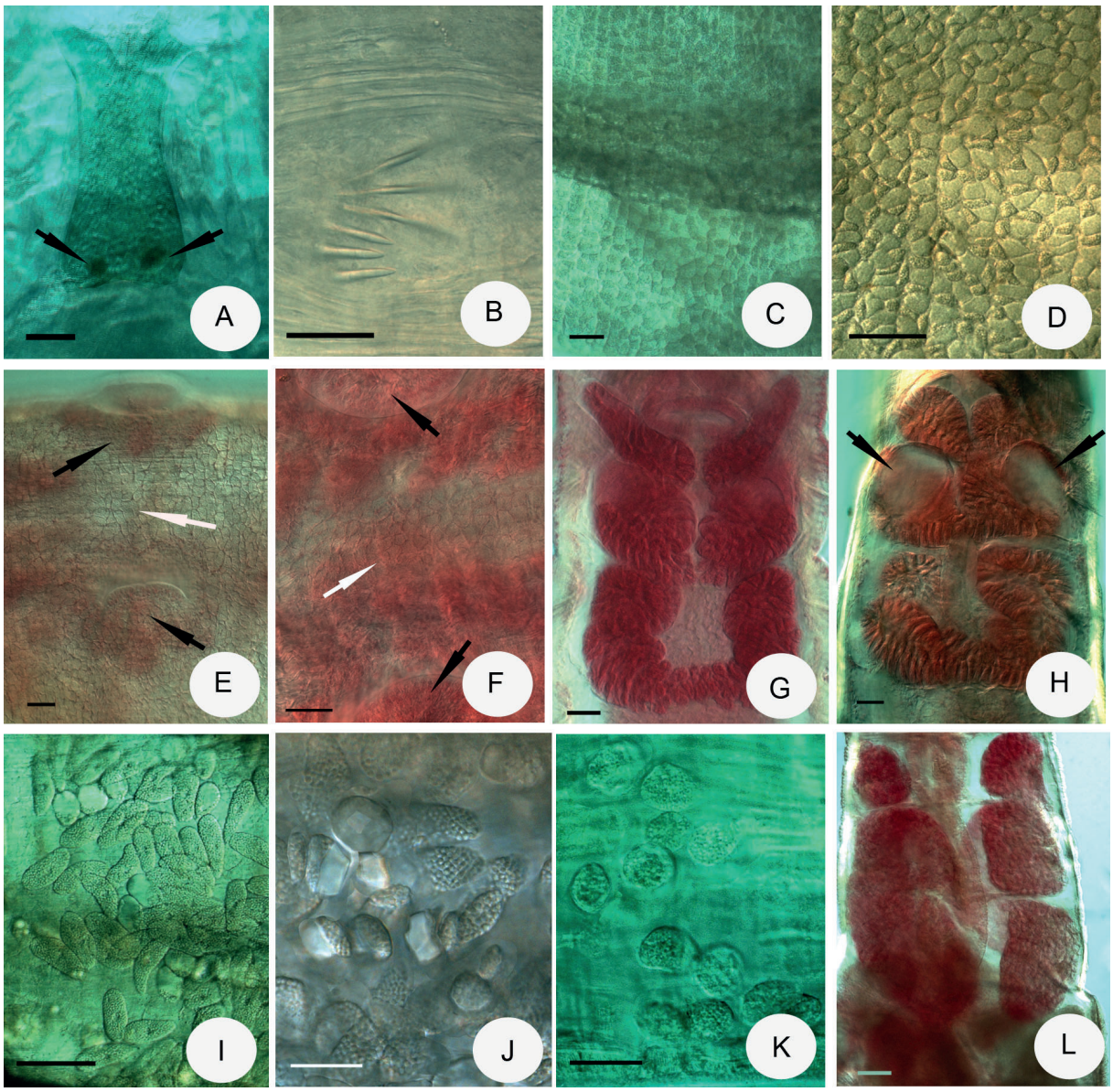

Fig. 2. Micrograph of *Enchytraeus adrianensis* sp. nov. **A–D, I–J**. In vivo. **E–H, K–L**. Fixed, stained. **A**. Brain (small aggregations of refractile globules marked with arrows). **B**. Chaetae in a ventral bundles with 3 surplus chaetae. **C**. Clitellar glands in regular rows. **D**. Clitellar glands in reticulate pattern. **E**. Paratype (slide 2748, P.143.3, ELTE). **F**. Slide 2684 (ELTE). **H**. Slide 2761 (ELTE). **K**. Paratype (slide 2851, P.143.10, ELTE). **L**. Paratype (slide 2760, P.143.6). **E–F**. Clitellar glands, ventral view (male copulatory organs marked with black arrow, between these organs the granulocytes marked with white arrows). **G**. Paratype (slide 2856, P.143.15, ELTE), first pharyngeal glands free dorsally. **H**. All pharyngeal glands connected dorsally (spermathecae marked with arrows). **I–K**. Coelomocytes (in J the small hyaline, refracting corpuscules also present). **L**. Large paired lobes of sperm sacs. Scale bars: A–I, K–L = 50 µm; J = 20 µm.

Sperm sacs. Two or three paired lobes of sperm sacs, very large, filling the coelom of IX / X–XI (Fig. 2L). Testes and sperm funnels in XI, ovaries, male pores and glands in XII.

Sperm funnels. 350–690 μm long in vivo (300–500 μm, fixed), 1.7–4 × as long as wide, collar narrower than funnel body (Fig. 3A). Vasa deferentia distinctly tripartite, long, extending into segments XV–XIX. After sperm funnel and before male opening, vasa deferentia slender and ciliated (20–40 μm wide in vivo and fixed equally), middle part thickened (50–95 μm wide) and unciliated (Fig. 3B).

Spermatozoa. 75–100 μm long, heads 20–30 μm, fixed.

Male copulatory organs. Male glands multiple: one large rounded primary bulb near male pore, and 6–9 smaller secondary glands, mostly 8 (usually 4–5 on each side, but sometimes 5 in one side and only 3 at other). Besides, near male opening in middle 2–3 smaller additional glands. Glands arranged roughly in semicircle around male pore and primary bulb (diameter 200–350 μm, fixed) (Fig. 3C–F). Primary bulb 60–125 μm long and 50–95 μm wide, secondary glands near to primary glands longer than outside ones (40–100 μm long and 20–50 μm wide). Male pores covered by lip-like folds (100–160 μm wide), ventral recess absent (all data in fixed specimens).

Spermathecae (Figs 1A, 3G–I). With ectal duct, ampulla without diverticula, separate openings into oesophagus. Spermathecal ectal pore at $^{4}/_{5}$. Ectal duct with different length (90–160 μm in vivo, 70–160 μm, fixed), covered with gland cells (70–117 μm widely in vivo and 60–100 μm widely, fixed). In most specimens, ectal duct near ampulla without glands for short stretch, length about 7–12 μm. Canal of ectal duct 6–9 μm wide, widening entad. Ampulla oval or spherical, about 70–115 μm wide and 75–150 μm long, with distinct, about 13–20 μm wide walls, lumen with masses of spermatozoa, ental duct very short, connecting laterally with oesophagus. 2–7 mature eggs present at a time.

Differential diagnosis

In the *Enchytraeus albidus* species complex as circumscribed in Erséus *et al.* (2019), the new species and two other species of which sequences are available (*E. albellus*, *E.* cf. *krumbachi*) have tripartite vasa deferentia. In *E. albellus*, the ductus is ciliated in its full length, whereas in the new species and in *E. krumbachi* the thickened middle part is not ciliated. Moreover, *E. albellus* is different, because its spermathecal ampulla is irregular sac-like with one smaller diverticulum dorsally, but in the new species the ampulla is oval or spherical with a well developed wall without diverticula.

The new species is closely related to *E. krumbachi* based on morphological and molecular data. Morphological similarity is primarily observable in the form of the spermatheca and the absence of the ventral recess of the clitellum. In both species the ampullae are without diverticula, but in *E. krumbachi* round and the diameter is slightly larger (70–140 μm in the Ligurian Sea specimens of *E. krumbachi* collected in this study but in the new species often oval and only 70–115 μm). Furthermore, the new species is bigger (segment number 51–84, body length 7.7–24.9 mm and 490–950 μm wide at clitellum vs segment number 40–66, body length 7–14 mm and 500–860 μm wide at clitellum, in vivo). No doubt, that the ventral recess absent in both species, but in the male copulatory organ the primary bulb about the same size in both species. In the new species mostly 8 long, narrower secondary glands are in a semicircle, around male pore and primary bulb, but in *E. krumbachi* the primary bulb is surrounded with very much smaller secondary glands. Although the molecular data also showed a close relationship between the two species, they still supported a certain species-level separation. *Enchytraeus polatdemiri* differs from the new species by its smaller size (segment number 40–55, length 7.5–11 mm and 410–580 μm wide at clitellum), and the sperm funnel is 5 × as long as wide (vs 1.7–4 × as long as in the new species) and the vasa deferentia are not tripartite, ciliated throughout, and mostly confined to XII (vs XV–XIX).

Enchytraeus moebii is similar to the new species in the form of the male apparatus (large primary bulb and smaller accessory glands especially on the basis of figure of Michaelsen (1886: fig. 3 pl. II), but the principal differences are that the vasa deferentia are not tripartite, ciliated throughout and the collar of sperm funnel is wider than the funnel body (vs collar narrower than funnel body in the new species).

Enchytraeus irregularis differs principally from the new species by the well developed diverticulum of the spermatheca, by the smaller primary bulb of male apparatus (diameter 40–80 µm vs 60–125 µm in the new species), and the vasa deferentia of *E. irregularis* are uniform, ciliated throughout and confined

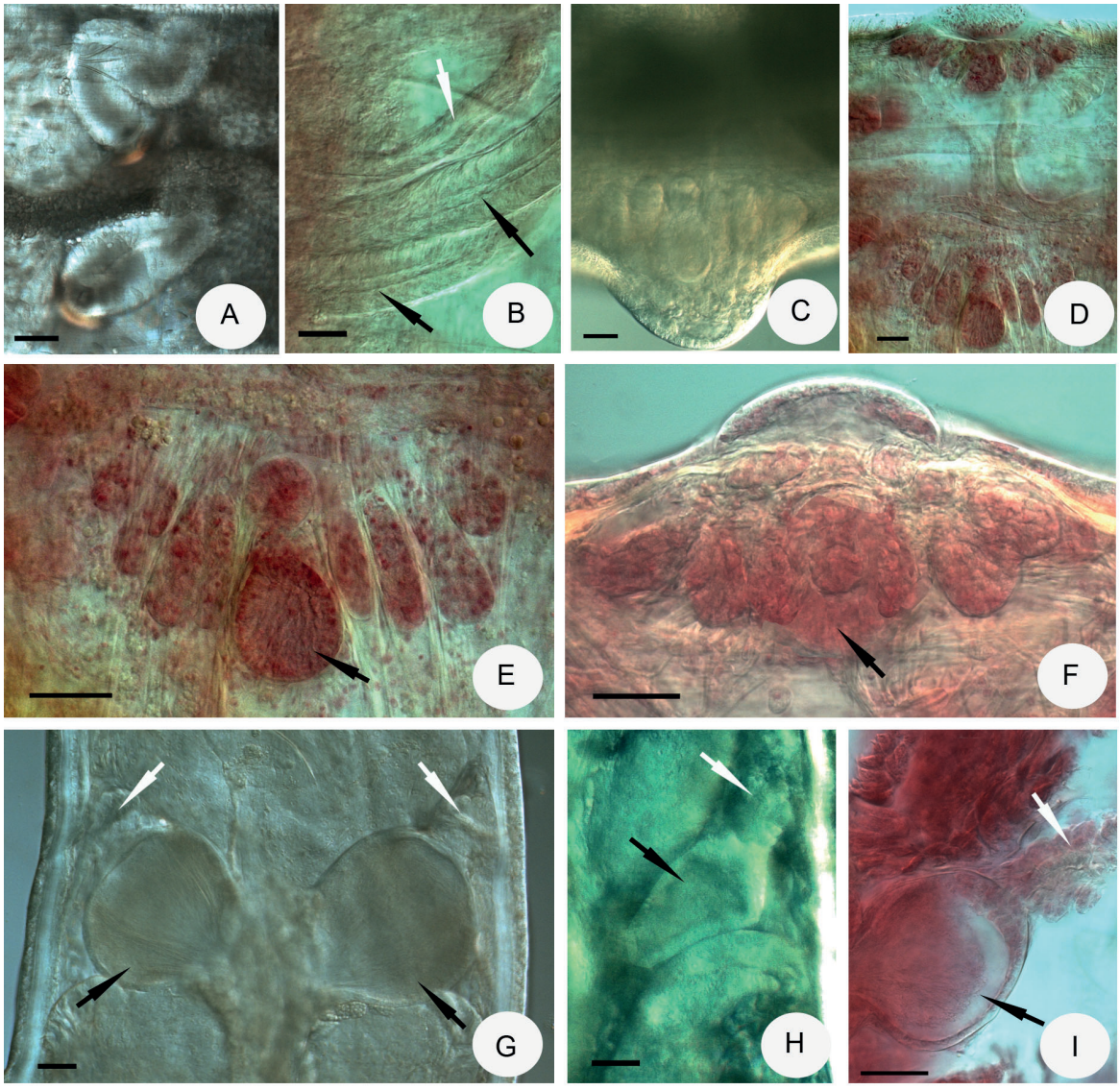

Fig. 3. Micrograph of *Enchytraeus adrianensis* sp. nov. **A, C, G–H**. In vivo. **B, D–F, I**. Fixed, stained. **A**. Sperm funnels. **B**. Paratype (slide 2748, P. 143.3, ELTE), sperm ducts (slender part marked with white arrow, wider part with black arrows). **C–F**. Multiple male glands (E–F primary bulb marked with arrow). **D**. Paratype (slide 2748, P.143.3, ELTE). **E**. Paratype (slide 2748, P.143.3, ELTE). **F**. Holotype (En.2. slide 2842, ELTE). **I**. Paratype (slide 2827, P. 143.8, ELTE). **F**. Holotype (En.2. slide 2842, ELTE). **G–I**. Spermathecae (ectal duct covered with glands marked with white arrows, ampullae filled with sperm in it marked with black arrows).Scale bars = 50 µm.

to XII. Very characteristic trait for *E. irregularis* is the oval or squarish glandular structure without external orifice ('accessory sexual glands') after or before male copulatory organs in XIII, XII or XI but in some specimens these organs may be absent.

For similarities and differences of the species of *Enchytraeus* studied by us, see Table 2.

Distribution and habitat

Kale Cove, Adriatic Sea, Kamenjak Peninsula, Istria, Croatia, decaying *Zostera* debris.

Enchytraeus andrasi sp. nov.
urn:lsid:zoobank.org:act:5E2BFD02-E8F8-4689-95F1-57E3A7B01A61
Figs 1C–D, 4, Tables 1–2

Diagnosis

(1) Body length 11–14 mm (in vivo), segment number 29–34; (2) chaetae maximum 3 per bundle, straight with ental hook; (3) clitellum in XII–XIII, hyalocytes and granulocytes irregularly arranged dorsally and laterally, ventrally absent between the male lip-like folds; (4) four pairs of nephridia preclitellarly; (5) all pharyngeal glands connected dorsally with ventral lobes, the third pair may be free; (6) dorsal blood vessel origin from XIV, blood colourless; (7) sperm funnel cylindrical, 380–580 μm long, 3–5 × as long as wide (in vivo); (8) vasa deferentia uniform, 24–25 μm wide with 8 μm thick wall (fixed), ciliated, not extending beyond XIII; (9) male glands multiple: one large rounded primary bulb, diameter 50–70 μm (fixed), and many smaller secondary glands; (10) spermathecal ectal duct (50–85 μm long, fixed) covered with gland cells, ampulla irregularly sac-like, about 100–106 μm wide with one large diverticulum (80–100 μm long, fixed), connecting with oesophagus; (11) more small mature eggs present at a time.

Etymology

Named in the honour of the brother of Klára Dózsa-Farkas, András Dózsa-Farkas, who collected the sample with this species.

Material examined

Holotype

ITALY • last 14 segments, 3.4 mm used for DNA analysis (No. 1386, ID number); Ligurian Sea, Castiglione seashore, decaying seagrass debris; 42°45′56.0″ N, 10°52′51.0″ E; 13 Dec. 2019; András and Kinga Dózsa-Farkas leg.; slide 2871, En.3; ELTE.

Paratypes

ITALY • 1 spec., last 9 segments, 1.65 mm used for DNA analysis (No. 1390, ID number); same collection data as for holotype; slide 2870, P.144.1; ELTE • 1 spec., last 9 segments, 1.65 mm used for DNA analysis (No. 1391, ID number); same collection data as for holotype; slide 2873, P.144.2; ELTE.

Description

Measurements. Medium-sized to large specimens. Holotype 14.3 mm long, 470 μm wide at VIII and 600 μm at clitellum in vivo, 9.3 mm long, 330 μm wide at VIII and 420 μm at clitellum, when fixed, 41 segments. Body length of paratypes 11–12 mm, width 430–450 μm at VIII and 550–680 μm at clitellum, in vivo. Length of fixed specimens 6.7–8.1 mm, width 420 μm at VIII and 470–580 μm at clitellum. Length of the first 12 segments 2.5–2.6 mm, after fixation. Segment number 29–34.

Table 2 (continued on next two pages). Comparison of morphological characters (measurements in fixed specimens). The data are derived from this study and from Erséus *et al.* (2019), Arslan *et al.* (2018) and according to the author of original species description (marked with*). The data given by us marked with bold, dimensions in µm.

Morphological characters	***E. adrianensis*** sp. nov.	***E. andrasi*** sp. nov.	***E. andrasiformis*** sp. nov.	***E.* cf. *krumbachi*** (Čejka, 1913), sensu Erséus *et al.* 2019	***E. irregularis*** Nielsen & Christensen, 1961*, sensu Dózsa-Farkas, 2019	***E. albidus*** s. str. Henle,1837, sensu Erséus *et al.* 2019	***E. polatdemiri*** Arslan & Timm, 2018	***E. möbii*** (Michaelsen, 1885), sensu Erséus *et al.* 2019	***E. albellus*** Erséus, Klinth & Rota, 2019
Segment number	**51–84**	**29–41**	**30–38**	65–75*, **40–66**	41–49*, **47–76**	**58–69**	40–55	60–74*	–
Length (mm)	**7.7–24, 9–28.2**	**6.7–9.3**	**9.6–13.4**	15*, **7–14**	**9–13**	**10–13**	7.5–11	25–35*	–
Length of 0–XII segm. (mm)	**2.2–4.8**	**2.5–2.6**	**3.4–4.4**	2.9–3.8, **2.7–3.8**	**2.3–3**	2.6–3.3, **2.6–2.8**	–	2.3–3.8	1.6–2.7
Diameter at clitellum	**490–950**	**470–580**	**540–720**	400–620, **500–860**	**530–880**	570–1080, **700–980**	410–580	430–890, 700–980*	510–720
Coelomocytes	**15–30**	**15–20**	**20–30**	10–15, **10–15**	**13–20**	10–20, **10–15**	20–30	10–15	10–25
Chaeta-number pre–postclitellarly, ventrally	**3,4–2,3**	**3–2,3**	**3, (4)–3,(2)**	3–4–2, **3–4,(5)–2,3**	**3–3**	3,4,5–2,3,4	2,3–2,3	3–4,(5)–2–3	3,4,5–2,3,(4)
Chaetae in clitellum dorsally	**2, 3**	**2**	**0, (2)**	2, **2, 3**	**2**	2, 3	2	2	0, 2
Origin of dorsal blood vessel	**XIV–XV**	**XIV**	**XIV**	?, XV*, **XV**	**XIV–XVI**	XIII–XVI	XII–XIV, (XV)	XIV–XV	XIV–XV
Colour of blood	**colourless**	**colourless**	**colourless**	colourless	**pink**	colourless/ yellowish	colourless	colourless	colourless
Length of sperm funnel	**300–500**	**235–330**	**220–470**	215–305, **200–560**	**270–600**	550–1085	–	295–420	400–530
Length : width ratio of sperm funnel	**1.7–4**	**2.0–2.5**	**3–4**	1.5–2, 3*, **1.2–3**	**2–4**	5–7	5	1.5–3.5	2–4
Relation of collar to diameter of sperm funnel	**narrower**	**narrower**	**as wide/wider**	**about as wide**	**as wide / wider**	about as wide	about as wide	wider*	–
Type of sperm-duct	**tripartite**	**uniform**	**uniform**	tripartite	**uniform**	uniform	uniform	uniform	tripartite
Diameter of duct, if uniform	–	**24–25**	**18–24**	–	**15–22**	30–55	30 µm near s.funnel, 15 µm near opening	20–25	–

Table 2 (continued).

Morphological characters	***E. adrianensis*** sp. nov.	***E. andrasi*** sp. nov.	***E. andrasiformis*** sp. nov.	***E.* cf. *krumbachi*** (Čejka, 1913), sensu Erséus *et al.* 2019	***E. irregularis*** Nielsen & Christensen, 1961*, sensu Dózsa-Farkas, 2019	***E. albidus*** s. str. Henle,1837, sensu Erséus *et al.* 2019	***E. polatdemiri*** Arslan & Timm, 2018	***E. möbii*** (Michaelsen, 1885), sensu Erséus *et al.* 2019	***E. albellus*** Erséus, Klinth & Rota, 2019
Diameter of thicker part	**50–95**	–	–	50–55, **55–75**	–	–	–	–	30–45–(65)
Diameter of thinner part	**20–32**	–	–	15–30, **20–37**	–	–	–	–	25–35–(45)
Ciliation of ducts	**in thinner part**	**throughout**	**throughout**	in thinner part	**throughout**	throughout	throughout	throughout	throughout
Posterior extension of duct	**XV–XVI–XIX**	**XII–XIII**	**XII**	XVI*, XVIII, **XIV–XIX**	**XII**	XIV–XX	XII (XIII–XV)	XV–XVI, XVII*	XVI–XXVIII
Sperm-sacs	**paired in IX–XI**	**paired in X–XI**	**paired in X–XI**	paired in IX–XI	**paired in VIII–XI**	paired in VIII–X	unpaired in X–XI	paired in X	paired in IX
Full diameter of male copulatory organ	**200–350**	**180–250**	**215–300**	**250–280**	**100–150**	**270–375**	–	–	–
Diameter of primary bulb	**60–125**	**50–70**	**80–120**	85–90, **70–90**	**70–100**	60–95, **65–70**	ca 100	110–180	70–120
Number of secondary glands	**8 + 2**	**many**	**many**	many	**many**	many	9	about 8*	many
Size of secondary glands (relative to primary bulb)	**smaller**	**smaller**	**smaller**	smaller	**smaller**	smaller/about same	smaller	much smaller	much smaller
Extra copulatory gland	**absent**	**absent**	**present (absent)**	absent	**present**	absent	absent	absent	absent
Length of spermathecal-duct	**70–160**	**50–85**	**62–125**	80–100, **70–155**	**87–110**	**100–125**	80–85	short or medium	–
Diameter of ectal-duct + glands	**60–100**	**50–75**	**60–95**	60–65, **50–75**	**60–95**	75–155, **60–115**	–	80–125	65–120,
Diameter of ampulla	**70–115**	**100–106**	**100–140**	95–125, **70–140**	**75–130**	75–215, **85–170**	120–150	80–90	(40)–100–215
Shape of ampulla	**round/oval**	**irregular sac-like**	**rounded**	round	**sac-like**	sac-like	–	rounded	irregular sac-like
Diverticulum	**absent**	**1 large + 1 smaller**	**1 large**	absent	**1 large**	1/more/absent, sack-like, **1 sack-like**	absent	absent	1 dorsal

Table 2 (continued).

Morphological characters	***E. adrianensis*** sp. nov.	***E. andrasi*** sp. nov.	***E. andrasiformis*** sp. nov.	***E.* cf. *krumbachi*** (Čejka, 1913), sensu Erséus *et al.* 2019	***E. irregularis*** Nielsen & Christensen, 1961*, sensu Dózsa-Farkas, 2019	***E. albidus*** s. str. Henle,1837, sensu Erséus *et al.* 2019	***E. polatdemiri*** Arslan & Timm, 2018	***E. möbii*** (Michaelsen, 1885), sensu Erséus *et al.* 2019	***E. albellus*** Erséus, Klinth & Rota, 2019
Max. length and diameter of chaetae preclitellarly	**72–112 × 5–7.5**	**60–62 × 5**	**65–75 × 4–5**	55–75 × 5 **60–95 × 6–7.5**	**70–100 × 6–7.5**	80–130 × 5–8 **110–100 × 6–7.5**	80–110 × 6–7	60–120 × 5–8	65–115 × 5–8
Max. length and diameter of chaetae postclitellarly	**70–100 × 5–7.5**	**67–75 × 4–5**	**67–85 × 4– 5**	**62–72 × 5–6**	**75–87 × 7–5**	slightly smaller **100–120 × 7–7.5**	same or slightly larger	–	slightly smaller
Mature eggs	**2–7**	**many**	**8–14**	4–10	**2–8**	3–8, **3–4**	–	1–5	1–4
Locality (country)	Croatia	Italy	Italy	Croatia*, Spain, Italy	Denmark*, Hungary, Korea	laboratory culture + see in Erséus *et al.* (2019)	Turkey	Germany*, Sweden, Norway, Spain, Denmark	Sweden, Norway, Greenland

Chaetae. Chaetal formula: 3–2,3:3–2,3. Chaetae straight with ental hook, about equal in size within bundle, 60–62 μm × 4 μm preclitellarly and 67–75 μm × 4–5 μm posteriorly. Often 2–3 surplus chaetae near bundles (Fig. 4B). Chaetae in XII absent ventrally, but present laterally, 2 per bundle.

Head pore. At 0/I.

Epidermal glands. Inconspicuous.

Clitellum. In XII–XIII, hyalocytes and granulocytes irregularly arranged dorsally and laterally (Fig. 4C), ventrally absent between male lip-like folds (Fig. 4E). Before and behind some glands but few.

Brain (Fig. 4A). About 1.8–2 × as long as wide, truncate posteriorly, sides slightly merging anteriad.

Oesophageal appendages. Pair of blind-ending tubes. In two specimens all primary pharyngeal glands connected dorsally, with ventral lobes (Fig. 4D), but in third specimen last pair free dorsally.

Dorsal blood vessel. From XIV, blood colourless. Anterior bifurcation in I.

Nephridia. Four pairs of preclitellar nephridia from 6/7–9/10, anteseptale funnel only, postseptale bulged, short efferent duct, originating postero-ventrally (Fig. 4F).

Coelomocytes. Oval, texture granulated, about 18–25 μm long, in vivo. No shining, hyaline corpuscles.

Subneural glands. Absent.

Sperm sacs. Two paired large lobes of sperm sacs, filling the coelom of X–XI. Testes and sperm funnels in XI, ovaries, male pores and glands in XII.

Sperm funnels. Large, 380–580 μm long, 3–5 × as long as wide in vivo (235–330 μm long and 2–2.5 × as long as wide, fixed). Collar slightly narrower than funnel body (Fig. 4H). Vasa deferentia long, irregularly coiled in XII–XIII, about 24–25 μm wide with 8 μm thick wall (fixed), ciliated (Fig. 4G, I).

Spermatozoa. Not measurable, heads about 21–36 μm, in vivo.

Male copulatory organs. Male glands multiple: one larger rounded primary bulb (diameter 50–70 μm, fixed) near male pore, and many smaller (32–78 μm long and 18–24 μm wide, fixed) secondary glands. Glands arranged roughly in semicircle around male pore and primary bulb (diameter 180–250 μm, fixed) (Fig. 4J). Male pores covered by lip-like folds (about 80 μm wide), recess present.

Spermathecae (Figs 1C–D, 4K). With short ectal duct (50–85 μm long, fixed), covered with gland cells (50–75 μm widely in vivo and fixed equally), canal 4–6 μm wide. Ampulla irregularly sac-like, about 100–106 μm wide, heads of spermatozoa embedded in wall of ampulla. Ampulla with one large diverticulum (80–140 μm long, 40–68 μm wide, fixed) (Fig. 1C), in one case ampulla also with small diverticula-like protrusions (Figs 1D, 4K). Ental duct short and opens into oesophagus separately. More small mature eggs present at a time (Fig. 4I).

Differential diagnosis

In the new species, like as in four of the species in the *E. albidus* complex (*E. albidus* s. str., *E. moebii*, *E. polatdemiri* and *E. irregularis* of which sequences are available, the vasa deferentia approximately uniform and ciliated throughout. The principal differences are that the spermathecal ampullae have diverticula in the new species but neither *E. moebii* nor *E. polatdemiri* have it. Besides *E. moebii* is much larger than the new species (body length 25–35 mm with segment number 60–74 vs 6.7–9.3 mm

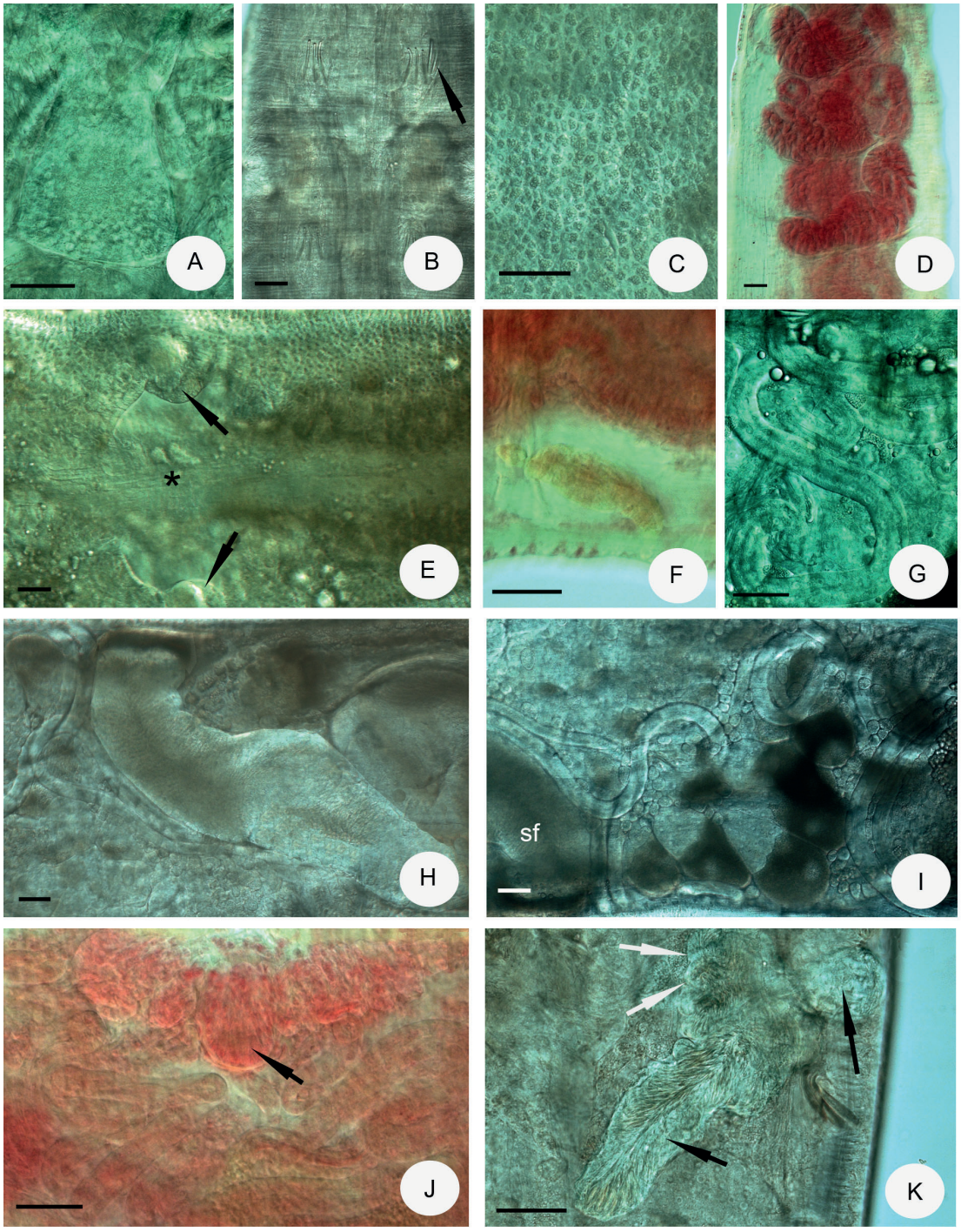

Fig. 4. Micrograph of *Enchytraeus andrasi* sp. nov. **A–C, E, G–I, K**. In vivo. **D, F, J**. Fixed, stained. **A**. Brain. **B**. Chaetae in ventral bundles preclitellarly (surplus chaetae marked with arrow). **C**. Clitellar glands of holotype, dorsal view. **D**. Paratype (slide 2870, P.144.1, ELTE), pharyngeal glands. **E**. Clitellar glands of holotype, ventral view (male lip-like folds marked with arrows, between the folds the glands absent: marked with *). **F**. Paratype (slide 2870, P. 144.1, ELTE), nephridium at $^{7}/_{8}$. **G**. Sperm duct. **H**. Sperm funnel. **I**. Sperm duct and many small eggs. **J**. Holotype (slide 2871, En.3, ELTE), multiple male glands of holotype (large primary bulb marked with arrow). **K**. Spermatheca (large diverticulum marked with short black arrow, small diverticula like protrusions marked with white arrows, ectal duct covered with glands marked with long, black arrow). Scale bars = 50 µm.

29–41) and has more chaetae in ventral bundle (4–5 vs 3). Although in *E. irregularis* the spermatheca has also diverticulum and the maximum number of chaetae is 3, but *E. irregularis* is larger than the new species (length 9–13 mm with segment number 47–76), and the blood is pink (in *E. andrasi* sp. nov. colourless) and has extra copulatory glands. Morphologically, *E. albidus* s. str. is most similar to the new species taking, the form of the spermatheca into consideration, but differs from it in size (10–13 mm with 58–69 segments vs 6.7–9.3 mm and 29–41 segments) and in the maximum number of chaetae (4–5 vs 3) and the sperm duct extends into XIV–XX (vs only in XII–XIII). The new species is also similar to *E. andrasiformis* sp. nov., with the morphological differences listed in the differential diagnosis of the latter species. As shown below, *E. andrasi* is clearly distinguished as separate from all other species by genetic data, which also give strong support for *E. andrasi* being most closely related to *E. andrasiformis*, described below.

For similarities and differences of the species of *Enchytraeus* studied by us, see Table 2.

Distribution and habitat

Castiglione seashore, Ligurian Sea, Italy, decaying seagrass debris.

Enchytraeus andrasiformis sp. nov.
urn:lsid:zoobank.org:act:F5887255-EE25-42BD-8035-40559810DCD1
Figs 1E, 5, Tables 1–2

Diagnosis

(1) Body length 13–19.5 mm (in vivo), segment number 30–38; (2) chaetae maximum 2–3 (4) per bundle, straight with ental hook; (3) clitellum in XII–XIII, hyalocytes and granulocytes irregularly arranged dorsally and laterally, but between the male lip-like folds ventrally absent; (4) four pairs of nephridia preclitellarly; (5) the first and second pairs of primary pharyngeal glands free dorsally with ventral lobes, third pair connected dorsally; (6) dorsal blood vessel origin from XIV, blood colourless; (7) sperm funnel variable large, 300–750 μm long, 4–7 × as long as wide in vivo; (8) vasa deferentia uniform, 18–24 μm wide with 5–7 μm thick wall (fixed), ciliated; (9) male glands multiple: one large primary bulb 80–120 μm long, 65–100 μm wide (fixed), and many smaller secondary glands. Often one additional sexual gland, rounded or oval (diameter 80–100 μm, fixed); (10) spermathecal ectal duct (62–125 μm long, fixed) covered with gland cells, ampulla spherical with one large diverticulum (90–200 μm long), ampulla connecting with oesophagus; (11) 8–14 small mature eggs present at a time.

Etymology

Named after its similarity to *Enchytraeus andrasi* sp. nov.

Material examined

Holotype

ITALY • Castiglione della Pescaia, Punta Ala Grosseto, decaying seagrass debris; András and Kinga Dózsa-Farkas leg.; 24 Sep. 2020; from culture: 1 Feb. 2021; En. 4, slide 3132; ELTE.

Paratypes

ITALY • 1 spec., last 9 segments, 2.5 mm used for DNA analysis (No. 1454, ID number); same collection data as for holotype; P. 145.1, slide 3093; ELTE • 1 spec., same collection data as for holotype; P.145.2, slide 3094; ELTE.

Description

Measurements. Medium-sized to large specimens. Holotype 13 mm long, 420 µm wide at VIII and 595 µm at clitellum in vivo (9.6 mm long, 440 µm wide at VIII and 540 µm at clitellum, when fixed), 38 segments. Body length of paratypes 14–19.4 mm, width 560–650 µm at VIII and 820–860 µm at clitellum in vivo. Length of fixed specimens 10.9–13.4 mm, width 550–610 µm at VIII and 630–720 µm at clitellum. Length of the first 12 segments 3.4–4.4 mm, after fixation. Segment number 30–34.

Chaetae. Chaetal formula: (2),3–3,2,1:3,(4)–3,(2). Four chaetae in the ventral bundles were observable only in one case. Chaetae straight with ental hook, about equal in size within a bundle, 65–75 µm × 4–5 µm preclitellarly and 67–85 µm × 4–5 µm posteriorly. Often found 2–3 surplus chaetae near the bundles (Fig. 5D). Chaetae absent in XII ventrally and laterally, but in one specimen present laterally.

Epidermal glands. Inconspicuous.

Clitellum. Girdle-shaped, in XII–XIII, (but in paratype slide 3093 in ½XI–¼XIII), hyalocytes and granulocytes irregularly arranged dorsally and laterally (Fig. 5B–C), absent between male lip-like folds in ventral recess (Fig. 5H). Before and behind this area clitellar cells present.

Head pore. At 0/I.

Brain (Fig. 5A). About 1.7–2.2 × as long as wide, truncate posteriorly, sides slightly merging anteriad.

Oesophageal appendages. Pair of blind-ending tubes. First and second pair of primary pharyngeal glands free dorsally with ventral lobes (Fig. 5E), but the third pair connected dorsally.

Dorsal blood vessel. From XIV, blood colourless. Anterior bifurcation near prostomium.

Nephridia. Four pairs of preclitellar nephridia from 6/7–9/10, anteseptale funnel only, postseptale bulged, efferent duct short, origin postero-ventrally.

Coelomocytes. Oval, texture granulated, about 30–36 µm long, in vivo [20–30 µm, fixed (Fig. 5F)], shining, hyaline corpuscles absent.

Subneural glands. Absent.

Sperm sacs. Two paired large lobes of sperm sacs, filling in all coelom of X–XI. Testes and sperm funnels in XI, ovaries, male pores and glands in XII.

Sperm funnels. Variably large, 300–750 µm long, 4–7 × as long as wide in vivo (220–470 µm long and 3–4 × as long as wide, fixed), collar of same width as funnel itself or slightly wider (Fig. 5G). Vasa deferentia uniform, irregularly coiled in XII, about 18–24 µm wide with 5–7 µm thick wall (fixed), slightly ciliated.

Spermatozoa. 105–130 µm long, heads about 28–48 µm, in vivo.

Male copulatory organs. Male glands multiple: one larger rounded primary bulb (80–120 µm long, 65–100 µm wide, fixed) and many smaller secondary glands (28–65 µm long, fixed). Secondary glands arranged roughly in semicircle around male pore and primary bulb, 215–300 µm in length, fixed. In holotype and one paratype (slide 3094), at one end of smaller glands of both male copulatory glands, one round (diameter 80–100 µm, fixed) extra sexual gland observable (Fig. 5H–I). In another paratype (slide 3093) these glands not observable. Male pores covered by lip-like folds (about 130 µm wide).

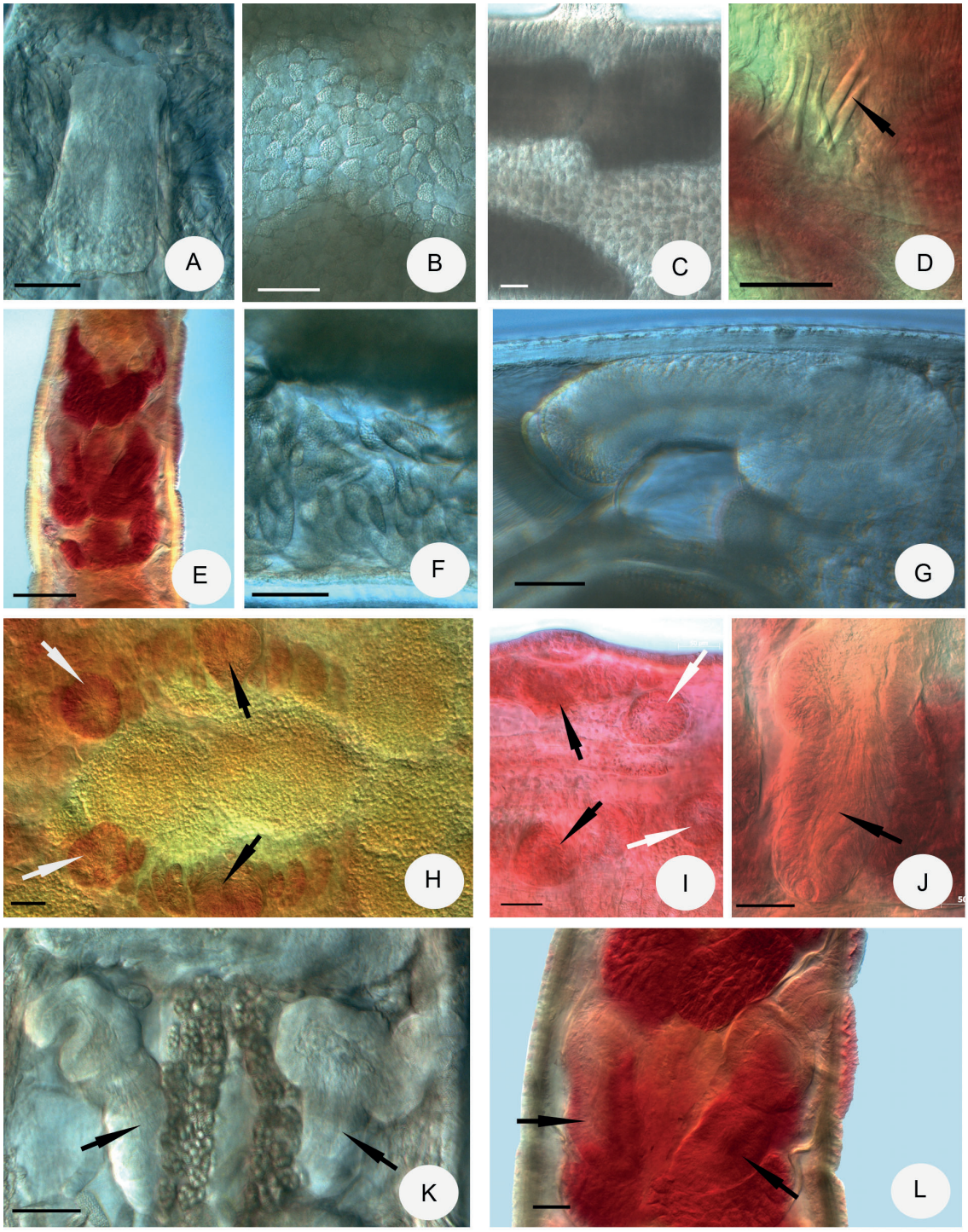

Fig. 5. Micrograph of *Enchytraeus andrasiformis* sp. nov. **A–C, F–G, I, K**. Holotype (slide 3132, En. 4; ELTE). **A–C, F–G, K**. In vivo. **D–E, H–J, L**. Fixed, stained. **A**. Brain. **B**. Clitellar glands, dorsal view. **C**. Clitellar glands, lateral view (three eggs visible). **D**. Paratype (slide 3094, P.145.2, ELTE), chaetae in ventral bundles with surplus chaetae, preclitellarly. **E**. Paratype (slide 3093, P.145.1, ELTE), pharyngeal glands. **F**. Coelomocytes. **G**. Sperm funnel. **H**. Paratype (slide 3094, P.145.2). **J**. Paratype (slide 3094, P.145.2, ELTE). **L**. Paratype (slide 3093, P.145.1, ELTE). **H–I**. Multiple male glands (large primary bulb marked with black arrows, extra sexual glands marked with white arrows). **J–L**. Spermathecae. Scale bars = 50 μm.

Spermathecae (Figs 1E, 5J–L). With short ectal duct (62–125 μm long, fixed), covered with gland cells (60–95 μm widely in vivo and fixed equally), canal 2.5–5 μm wide. Ampulla spherical (diameter 100–140 μm) with one large diverticulum (90–200 μm long and 40–100 μm wide, fixed), separate openings into oesophagus. More (8–14) small mature eggs present at a time.

Differential diagnosis

The new species, like *E. andrasi* sp. nov., differs from the other species of the *E. albidus* complex (see in the differential diagnosis of *E. andrasi*) and very similar to *E. andrasi* morphologically, but can be considered as two separate species based on the results of molecular analysis. Some morphological differences also supported this distinction. Both species is about as long as *E. albidus* s. str. (10–13 mm vs 9.6–13.4 mm for *E. andrasiformis* sp. nov. and 6.7–9.3 mm long for *E. andrasi* sp. nov.) however the two new species are slightly thinner than the latter, width at clitellum (fixed) being 420–580 μm for *E. andrasi*, 540–720 μm for *E. andrasiformis*, 700–980 μm for our new material of *E. albidus*, and even up to 1080 μm for *E. albidus* studied by Erséus *et al.* (2019). The coelomocytes in *E. andrasiformis* are larger (30–36 μm long) but 18–25 μm in *E. andrasi* sp. nov. in vivo, (20–30 μm vs 15–20 μm, fixed), the sperm funnel is also larger (220–470 μm long vs 235–332 μm long, fixed) and the collar has the same width or slightly wider as the funnel body in *E. andrasiformis*, but narrower than funnel body in *E. andrasi*. The male copulatory organs of the two species are similar, but in *E. andrasiformis* the primary gland is slightly larger (Table 2), furthermore, two extra sexual glands were observed in two out of three specimens. Finally, in *E. andrasiformis*, the two anterior pairs of primary pharyngeal glands not united dorsally, only the third pair, whereas both of the first and second pairs are united dorsally and the third pair either united or free in *E. andrasi*. Additional morphological data for some species of the *Enchytraeus albidus* complex is similar as in *E. andrasi*.

For similarities and differences of the species of *Enchytraeus* studied by us, see Table 2.

Distribution and habitat

Punta Ala Grosseto, Castiglione della Pescaia, Italy, decaying seagrass debris.

Morphological notes on further new material included in this study

Enchytraeus albidus Henle, 1837 s. str.
Figs 1F, 6, Tables 1–2

Material examined

HUNGARY • 16 specs; Budapest; ID 1300 to 1301, 1461 to 1462, slide 3012, 3013, 3016 to 3018, 3024, 3028, 3044 to 3048; ELTE.

Description of new material

We investigated a living population of *E. albidus* s. str. from the laboratory of Szent István University, Hungary, which was derived from the culture of ECT Oekotoxikologie GmbH, Flörsheim, Germany. From this culture the neotype of *E. albidus* has been selected (Erséus *et al.* 2019). In this way our morphological characters substantially agree with those described in Erséus *et al.* (2019).

Measurements. Segment number 58–65, body length 15.5–20.8 mm, 850–900 μm wide at clitellum in vivo (700–980 μm, when fixed).

Chaetae. In ventral bundles mostly 3–5 (Fig. 6A).

Brain. 125–165 μm long, 1.2–1.8 × as long as wide (fixed).

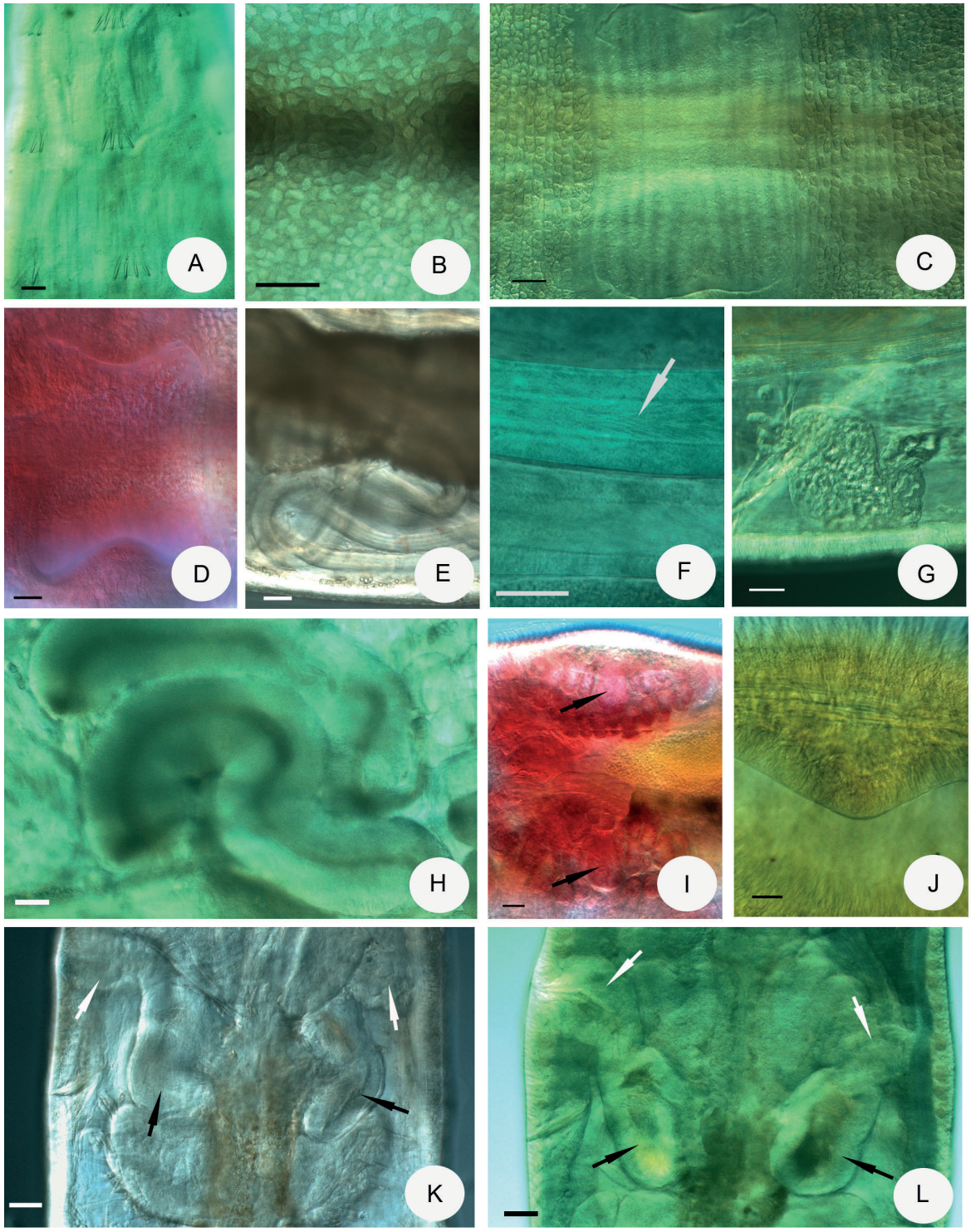

Fig. 6. Micrograph of *Enchytraeus albidus* Henle, 1837 s. str. **A–C, E–H, K–L**. In vivo. **D, I**. Fixed, stained. **J**. Fixed, not stained. **A**. Chaetae in ventral bundles preclitellarly. **B**. Clitellar glands, dorsal view. **C–D**. Ventral recess between the lip-like folds in XII. **D**. Slide 3047 (ELTE). **E–F** Sperm ducts (In F the ciliated canal marked with arrow). **G**. Nephridium. **H**. Sperm funnel. **I**. Multiple male glands (larger primary bulb marked with arrows) (slide 3048, ELTE). **J**. Lip-like fold (slide 3028, ELTE). **K–L**. Spermathecae (diverticula marked with black arrow, glands at ectal duct marked with white arrow). Scale bars = 50 µm.

Pharyngeal glands. Variable, all converging or connected dorsally, or not converging (in Erséus *et al.* 2019: all converging).

Coelomocytes. 17–32 μm long, mostly oval or spindle-shaped, granulated (in Erséus *et al.* 2019: 10–20 μm). In the coelomocytes mostly shining, hyaline, round or tetragonal corpuscles (diameter 9–15 μm) are also present, similar to *E. adrianensis* sp. nov.

Clitellum. Hyalocytes and granulocytes of clitellum irregularly arranged dorsally (Fig. 6B). Ventral surface of XII with a recess between lip-like folds (Fig. 6C–D, J).

Nephridia. Four pairs of nephridia preclitellarly (Fig. 6G).

Sperm funnels. 700–820 μm long in vivo, 5–6 × as long as wide, the collar as wide as funnel body (Fig. 6H). Head of spermatozoa 30–60 μm long. Sperm duct ciliated (Fig. 6E–F), elongate, about the same width throughout (30–44 μm wide, with 9–16 μm thick wall), coiled, extending into XIV–XVII.

Male copulatory organs. Male glands multiple: one larger rounded primary bulb (65–80 μm, fixed) and numerous smaller glands (40–50 μm, fixed) (Fig. 6I).

Spermathecae. Ectal duct of spermatheca 105–200 μm long, diameter of glands around duct 90–130 μm in vivo. Diverticulum of ampulla 180–237 μm long and 70–125 μm wide in vivo (Figs 1F, 6K–L).

For similarities and differences of the species of *Enchytraeus* studied by us, see Table 2.

Distribution and habitat

Laboratory culture. For additional references, including synonymies and further distributional data, see Erséus *et al*. (2019).

Enchytraeus krumbachi (Čejka, 1913)
Figs 1B, 7–8, Tables 1–2

Enchytraeus krumbachi Cejka, 1913: 145–151, figs 1–10.

Enchytraeus krumbachi – Erséus *et al.* 2019: 126–129, fig. 12.

Emended diagnosis

As a result of our comparisons, we suggest the following diagnosis of the species:

(1) Body length 15–25 mm (in vivo), segment number 40–66; (2) chaetae maximum 4 (5, 6) per bundle; (3) granulocytes and hyalocytes irregularly arranged dorsally in clitellum; (4) four pairs of nephridia preclitellarly; (5) the pharyngeal glands are connected dorsally; (6) dorsal blood vessel origin from XV, blood colourless; (7) sperm funnel 1.2–3 × as long as wide (fixed); (8) vasa deferentia tripartite, extending into XIV–XIX, the middle part thicker, unciliated, the thinner part ciliated; (9) male copulatory organs: one large rounded primary bulb, slightly longer than wide (80–100 μm × 70–90 μm), many smaller secondary glands; (10) ampulla of spermatheca rounded, large, without diverticula, ectal duct with large glands covered; (11) 4–10 mature eggs present at a time.

For similarities and differences of the species of *Enchytraeus* studied by us, see Table 2.

Material examined

ITALY • 11 specs (+ 12 specs only in vivo); Castiglione seashore; ID 1383, 1385, slide 2867 to 2869, 2872, 3004, 3006 to 3007, 3014 to 3015; ELTE • 3 specs; Punta Ala Grosseto; slide 3174, 3180 to 3181; ELTE.

Description of new material and comparison with previous accounts

Morphological characters identical with the description by Čejka (1913) and Erséus *et al.* (2019). Unfortunately, we did not have the opportunity to study the type material, but the original description is quite detailed and can be compared with our own data.

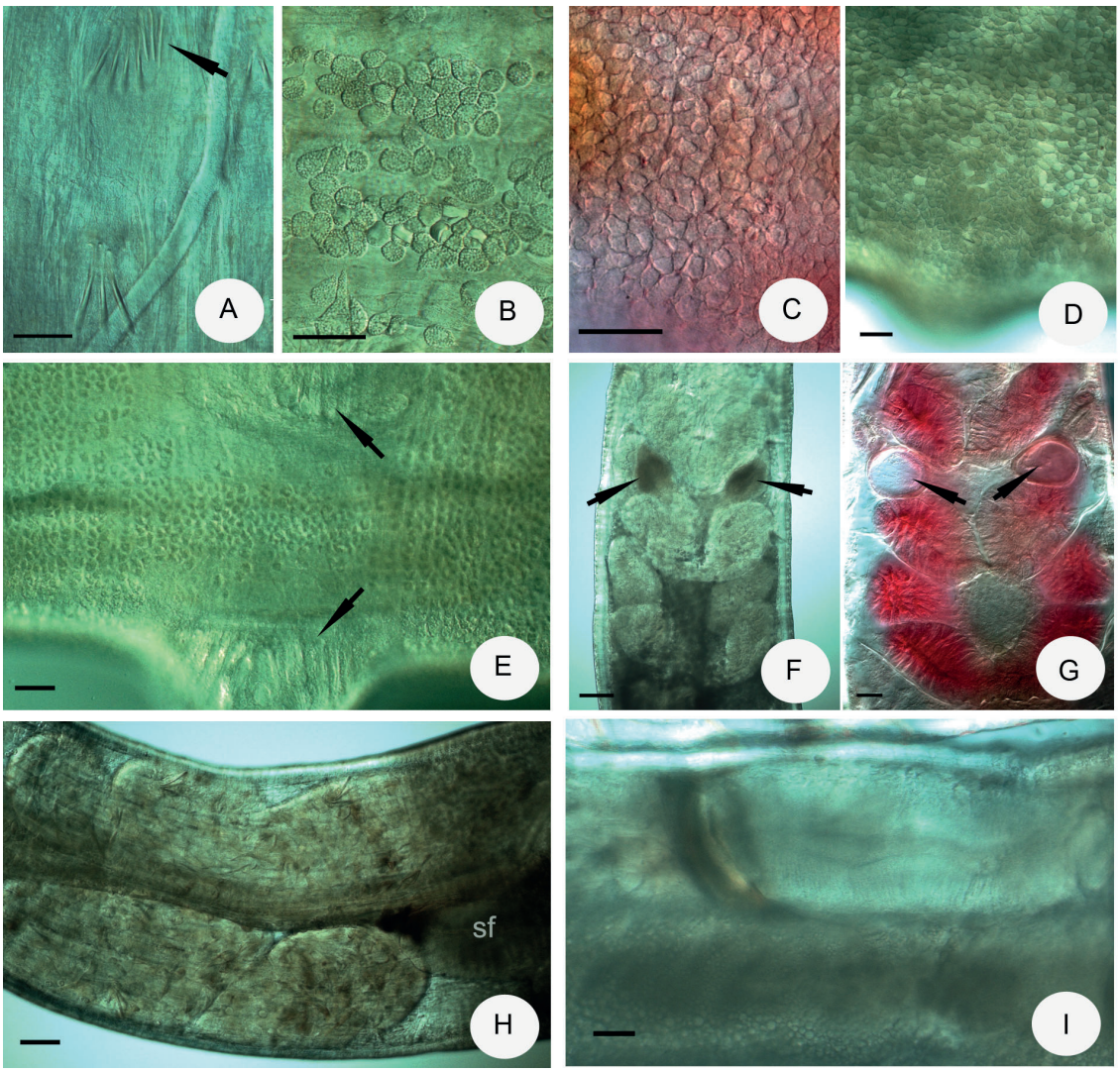

Fig. 7. Micrograph of *Enchytraeus krumbachi* (Čejka, 1913). **A–B, D–F, H–I**. In vivo. **C, G**. Fixed, stained. **A**. Chaetae in ventral bundles preclitellarly (surplus chaetae marked with arrow). **B**. Coelomocytes. **C**. Clitellar glands, dorsal view (slide 2868, ELTE). **D**. Clitellar glands, lateral view (near to male copulatory apparates more granular glands). **E**. Between the two male copulatory apparates (marked with arrows) and middle ventrally only granulocytes. **F–G**. Pharyngeal glands (in F first and secondary glands connected dorsally, in G these glands near to each other but not connected dorsally, the spermathecae marked with arrows). **G**. Slide 2867 (ELTE). **H**. Sperm sacs in X–XI. **I**. Sperm funnel. Scale bars = 50 µm. Abbreviation: sf = sperm funnel.

Measurements. Segment number 40–66. In vivo, body length 15–25 mm, width at clitellum 700–950 µm; when fixed, length 7–14 mm (with first 12 segments 2.7–3.8 mm), width 500–860 µm. Čejka (1913) originally reported 66–75 segments, and body ca 15 mm long, and Erséus *et al.* (2019), studying fixed worms, noted length of 2.9–3.8 mm for first 12 segments, and width of 400–620 um at clitellum. Thus, our specimens are roughly identical in general size to earlier studied material, although slightly wider than individuals examined by Erséus *et al.* (2019).

Chaetae. Chaetal formula: 2,3–2,3:2,3,4,(5,6)–2,3. In ventral preclitellar bundles of some specimens 3 chaetae, and only one or two bundles with 4 chaetae, in other specimens 4 chaetae in all or most bundles; sometimes 2–3 surplus chaetae can be found. In Erséus *et al.* (2019), chaetal formula 3–2:3,4–2 and

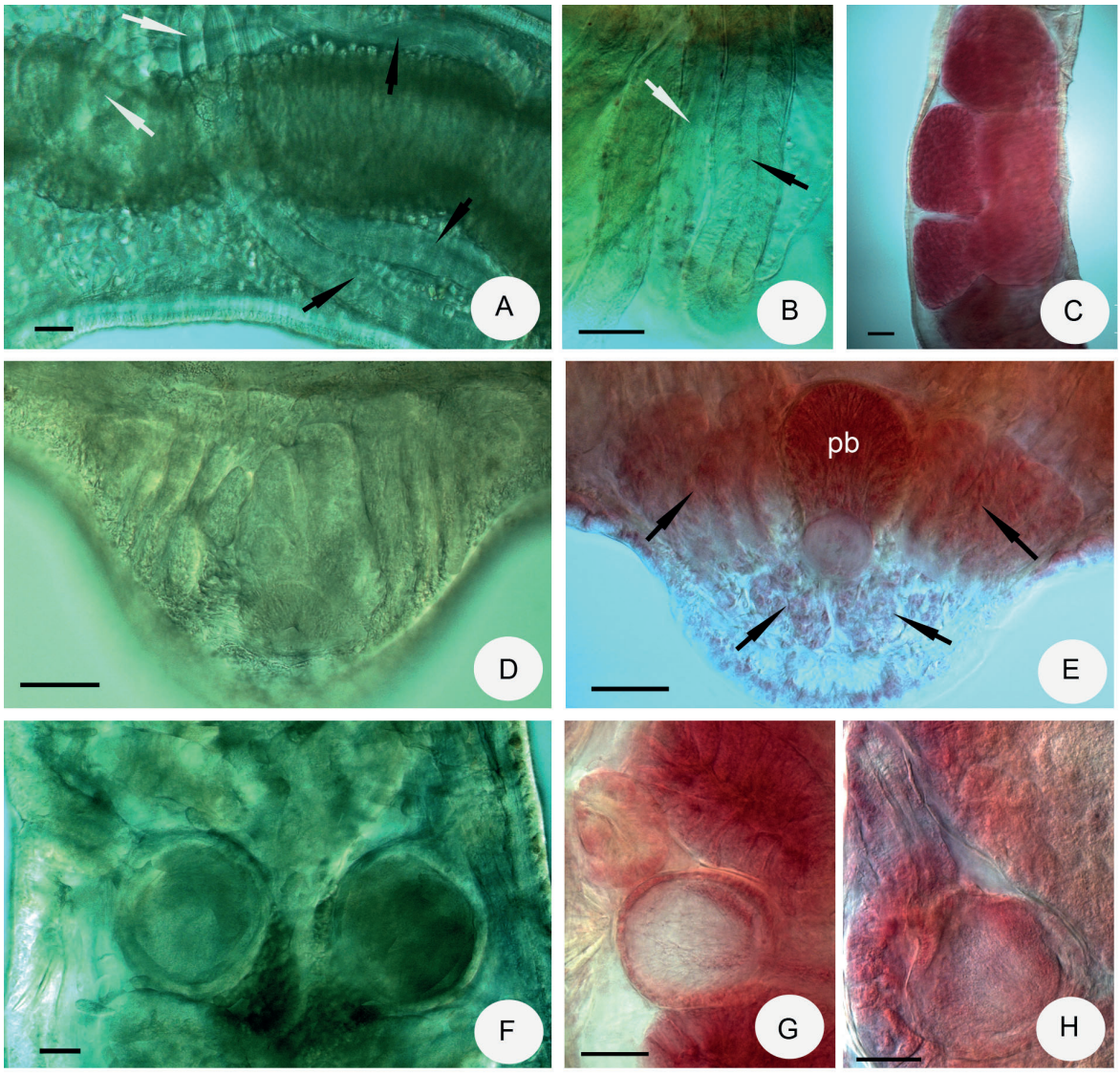

Fig. 8. Micrograph of *Enchytraeus krumbachi* (Čejka, 1913). **A–B, D, F**. In vivo. **C, E, G–H**. Fixed, stained. **A–B**. Sperm ducts (thick-wall portion marked with black arrow, thin-wall portions marked with white arrows). **C**. Large sperm sacs with more lobes (slide 2868, ELTE). **D–E**. Male copulatory apparates (many accessory glands marked with arrows). **E**. Slide 2868 (ELTE). **F–H**. Spermathecae (ampulla rounded without diverticula). **G**. Slide 2867 (ELTE). **H**. Slide 2872 (ELTE). Scale bars = 50 µm. Abbreviation: pbc = primer gland.

there are always 2 chaetae per bundle postclitellarly. Some of our individuals with 3 chaetae per bundle postclitellarly. In one specimen, 5 and 6 chaetae occured in some preclitellar ventral bundle. Čejka mentioned 3 chaetae in lateral and 4 chaetae in ventral bundles. Size of chaetae similar to size given by Erséus *et al.* (2019) (Table 2). 2–3 surplus chaetae also occasionally occur (Fig. 7A).

Coelomocytes. Round or narrowed at one end, texture granulated, 15–27 μm length in vivo (Fig. 7B), (fixed not well measurable) Erséus *et al.* (2019): 10–15 μm, fixed. Shining, hyaline corpuscles mostly absent, but in some specimens occuring in few numbers.

Clitellum. Granulocytes and hyalocytes irregularly arranged dorsally (Fig. 7C). In Erséus *et al.* (2019), ventral surface of XII with invaginations creating two recesses with overhanging lips. In our specimens near to male copulatory glands laterally (Fig. 7D) and ventrally between lips and midventrally only granulocytes (Fig. 7E). Čejka (1913) does not give any description of epidermal gland cells of epidermis.

Pharyngeal glands. In Erséus *et al.* (2019), pharyngeal glands are connected dorsally, in our individuals the position is mostly the same (Fig. 7F), but sometimes the first and second pairs of primary pharyngeal glands did not connect or they just contacted (Fig. 7G). In an unusual way, the third pair of pharyngeal glands was completely absent in one specimen.

Nephridia. Four pairs of preclitellar nephridia at 6 / 7–9 / 10.

Sperm funnels. Length: width ratio of sperm funnel (Fig. 7I) 1.2–3:1 (fixed), (Erséus *et al.* 2019: 1.5–2:1, Čejka 1913: 3:1). Vas deferens (Fig. 8A–B) has same structure, tripartite, middle part thicker (55–75 μm with 20–30 μm wall thickness), unciliated, thinner ductus 20–37 μm thick and ciliated. Sizes of thicker part of ductus slightly larger than given by Erséus *et al.* (2019) (50–55 μm, with 15 or 15–30 μm wall thickness). In Erséus *et al.* (2019), vas deferens reaches XVIII, in our specimens variable: XIV–XIX, in Čejka (1913), it reaches XVI.

Sperm sacs. Well developed, paired sperm sacs (Figs 7H, 8C) in IX–XI.

Male copulatory organs. One large rounded primary bulb, slightly longer than wide (80–100 μm × 70–90 μm), according to Erséus *et al.* (2019): diameter 85–90 μm and many smaller secondary (accessory) glands (Fig. 8D–E). In Čejka (1913), 6 gland complexes around penial bulb.

Spermathecae (Figs 1B, 7F–G, 8F–H). Without diverticula, ampulla round, large [70–140 μm, in Erséus *et al.* (2019): 95–125 μm], ectal duct with large glands covered (Figs 1B, 8F–H). In Erséus *et al.* (2019), ectal duct of spermatheca entally opening into small rounded chamber but we did not observe this chamber, and it is not mentioned in Čejka's original description. Besides, differences in length and diameter of ectal duct (see Table 2). According to the morphological comparisons above, we think that our specimens agree better with the morphological description of Čejka (1913).

Distribution and habitat

Castiglione seashore, Ligurian Sea, Italy, decaying seagrass debris. Punta Ala Grosseto, Castiglione della Pescaia, Italy, decaying seagrass debris.

Enchytraeus irregularis Nielsen & Christensen, 1961
Figs 1G, 9, Tables 1–2

Enchytraeus irregularis Nielsen & Christensen, 1961: 13.

Enchytraeus irregularis – Hong & Dozsa-Farkas 2018: 81–85, figs. 2–4.

Enchytraeus irregularis – Dózsa-Farkas K. 2019: 81–82, fig. 6.39.1

Material examined

KOREA • 5 specs; Jeollabuk-do, Songcheon-dong; ID: 262, 906, slide 573 to 575; ELTE.

HUNGARY • 5 specs; Érd; ID 946, slide 3029 to 3031, 3034 • 2 specs; Tiszalök, slide 2110 to 2111; ELTE.

Description

The species was described by Nielsen & Christensen (1961) from compost heap in the Botanical Garden of Copenhagen, Denmark. In 1987, Dózsa-Farkas found it in an earthworm-farm in Tiszalök (Hungary) and in 2016, in a sewage-sludge compost-bed in Érd (Hungary). In 2007, individuals of *E. irregularis* were collected from an earthworm breeding box in house (Korea, Jeollabuk-do) and a culture was made from these specimens. The results of the latter study were published in Hong & Dózsa-Farkas (2018). Schmelz & Collado (2010) proposed its synonymy with *E. capitatus* von Bülow, 1957, but Dózsa-Farkas (2019) disagreed with it. Now we were able to study these specimens using DNA sequencing, so all earlier specimens and some new specimens from Korea and Hungary were studied again morphologically. On the basis of the result of this new study, we give an additional description of this species.

Measurements. Body length 14–20 mm, width 540–700 μm at clitellum in vivo (length 9–13 mm and 530–880 μm wide, if fixed), segment number 47–66 (segment number 41–49 in Nielsen & Christensen 1961). Length of the first 12 segments 2.3–3.0 mm, after fixation.

Chaetae. Straight or slightly curved, formula of 3–2,3 : 3–2,3,(4).

Clitellum. Saddle-shaped, over XII–XIII (XIV), gland cells small, irregularly scattered (Fig. 9B).

Head pore. At 0/1.

Brain. About 150 μm long, 1.6 × as long as wide in vivo, with one or two pairs of aggregations of refractile globules (Fig. 9A).

Oesophageal appendages. Short, outline irregular, thin-walled with single central lumen. All three pairs of primary pharyngeal glands with connection dorsally and ventral lobes.

Dorsal vessel. From XIV–XVI, blood faintly red, anterior bifurcation in peristomium (Fig. 9D).

Coelomocytes. One type, only mucocytes, small, oval or elongate, pear-shaped, 20–29 μm long in vivo, filled with light granules (Fig. 9C). Shining hyaline corpuscles also occur but in few numbers.

Nephridia. Four pairs of nephridia preclitellarly.

Sperm sacs. Paired, well developed and lobed, located in IX–XI (Fig. 9G).

Sperm funnels (Fig. 9G). 415–730 μm long, 4–7 × as long as wide, about as long as the body diameter in vivo, (270–600 μm long, 2–4 × as long as wide, if fixed), collars slightly wider than funnel.

Spermatozoa. About 80–100 μm long, heads about 30 μm in vivo, sperm ducts uniform, about 20 μm wide.

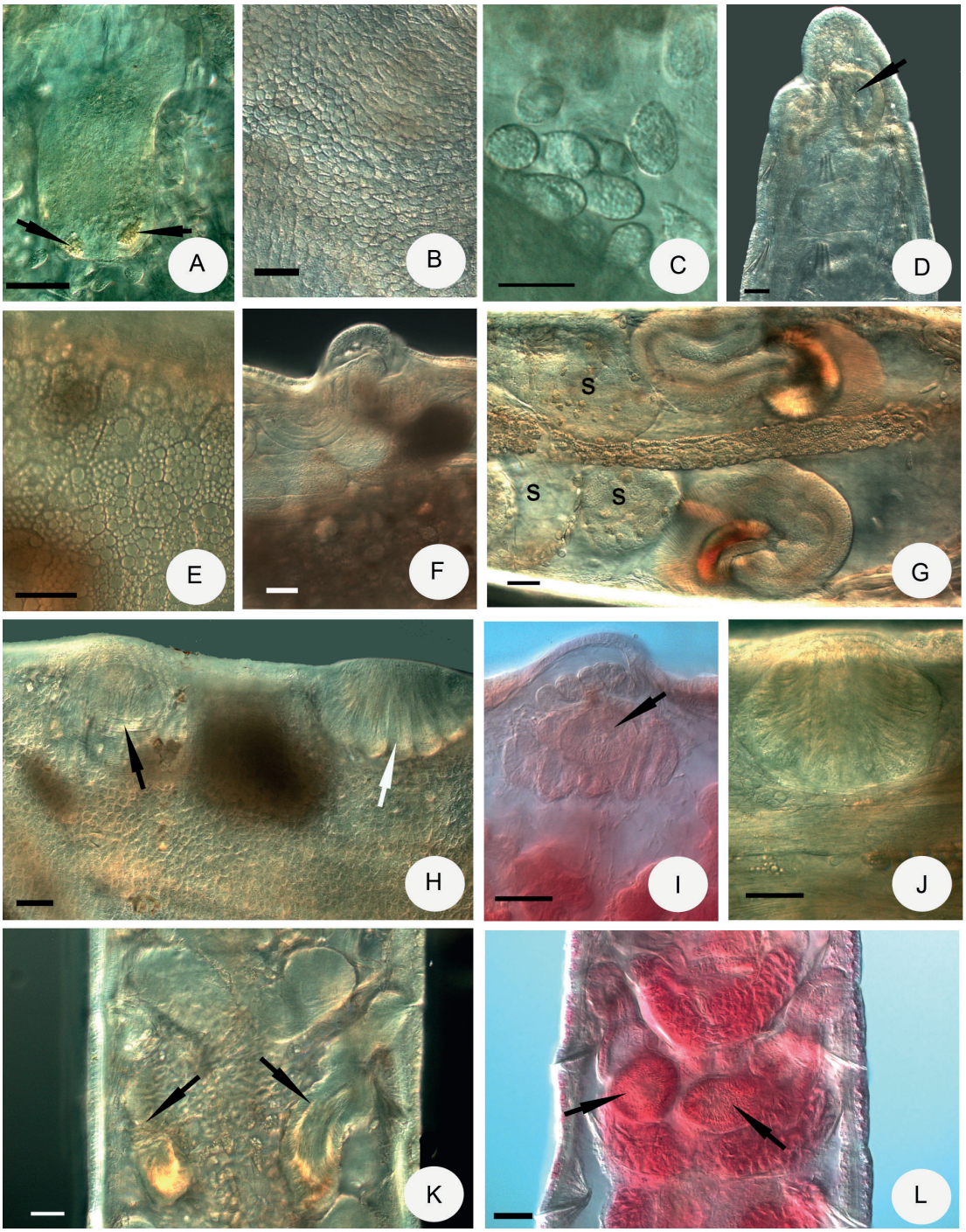

Fig. 9. Micrograph of *Enchytraeus irregularis* Nielsen & Christensen, 1961. **A–H, J, K**. In vivo. **I, L**. Fixed, stained. **I**. Slide 2110 (ELTE). **L**. Slide 574 (ELTE). **A**. Brain (refractile globules marked with arrows). **B**. Clitellar glands, dorsolateral view. **C**. Coelomocytes. **D**. Head, anterior bifurcation of blood vessel with red blood (head pore marked with arrow). **E**. Chloragogen cells. **F**. Male copulatory organ (lateral view). **G**. Sperm funnels. **H**. Segments XII–XIII (male copulatory organ marked with black arrow, extra sexual gland marked with white arrow). **I**. Multiple copulatory glands (lateral view, primary gland marked with arrow). **J**. Extra sexual glands in XIII, ventro-lateral view. **K–L**. Spermathecae (diverticula marked with arrows). Scale bars: A–B, D–L = 50 µm; C = 20 µm. Abbreviation: s = sperm sacs.

Male copulatory organs. Male glands multiple with larger primary bulb (70–100 µm × 70–100 µm) and 6–8 narrower, long, glandular secondary glands (50–90 µm × 12–14 µm) around male pores (Fig. 9F–G). After male copulatory organs pair of oval or squarish glandular structure visible with subdivision ('accessory sexual glands') (150–250 µm long, 110–225 µm wide, about 100 µm high, fixed), without external orifice (Fig. 9F, H–I). Usually in XIII, directly before the ventral chaetal bundles. In one specimen, visible immediately before male copulatory organs, and in another specimen, where clitellum was from XII to XIV, this organ was found in XV and only on one side (slide no. 573). Now revised again under microscope, so Hong & Dózsa-Farkas (2018): 85 is not correct: "clitellum extended over XII–XV and accessory sexual gland found in XIV" (but correct caption of fig. 3g). In Nielsen & Christensen (1961), location of this organ in front of penial bulb and also in XIII ventrally. These organs mostly larger than male copulatory organ.

Spermathecae. Spermathecal ectal ducts (87–110 µm long), with distinct canals (5–8 µm wide) and ring of glands around ectal orifices. Length of glands about 55–75 µm (fixed). Length of duct without glands proximally 13–25 µm. Duct widens into ampulla proximally (diameter of ampullae about 75–130 µm), which again gradually tapers into short ental ducts, communicating separately with oesophagus. From ampullae anteriorly or laterally arises one large diverticulum (170–220 µm long in vivo, 100–200 µm fixed) filled with spermatozoa (Fig. 9K–L). 2–8 mature eggs at a time.

Differential diagnosis

The main differences between this species and the other species investigated by us are the pink blood, and the characteristic large extra sexual glands without external orifice.

For similarities and differences of this species compared to other species of the *E. albidus* complex, see Table 2.

Distribution and habitat

Songcheon-dong, Jeollabuk-do, Korea, earthworm breeding box in house. Tiszalök, Hungary, earthworm-farm. Érd, Hungary, sewage-sludge compost bed. This species has unknown origin, only appeared in culture, it has not yet been found in the wild.

Enchytraeus sp.2 and Enchytraeus sp.3 (Enchytraeus cf. kincaidi Eisen, 1904?)

In 1993, enchytraeids were collected from Spitzbergen (Svalbard) and Birkemoe & Dózsa-Farkas (1994) give a short description about the worms. These worms were identified by them as *E. kincaidi* Eisen, 1904, on the basis of Coates & Ellis (1981), primarily because of the maximum of 3 chaetae in the ventral bundles and the presence of the glands only at the spermathecal ectal ducts orifice, not covered along the duct. Later (in 2000), Birkemoe sent some living specimens to Dózsa-Farkas, who made a culture. From this culture, some specimens were fixed in 70 % ethanol and freezed for DNA study. Also in 2000, Yves Frenot sent some fixed specimens from the Kerguelen Islands to Dózsa-Farkas, and they were identified as *E. albidus* sensu lato. Now we tried to make new preparations from the old material, but they were not suitable. Therefore, we can only give a brief morphological description. According to the molecular results of specimens from Spizbergen and Kerguelen Islands, they seem to be the same species (see results of molecular analysis), at the same time they differed from the other molecular data of the *E. albidus* group known so far. We include these findings to this study to point out, that the *E. albidus* complex is very diverse along its wide distribution, and the occurrence of additional new species is expected. If it will be possible to collect new material, then it will be possible to perform more precise morphological investigations and decide in the future, whether they are the same as *E. kincaidi*. Because the Svalbard and Kerguelen specimens are very close to each other on the gene trees, probably they belong to the same species (see Figs 10–11) so we present them as *E.* sp.2 / sp.3 on the species tree.

Enchytraeus sp.2 from Svalbard

Material examined

SVALBARD • 7 specs; Kongsfjorden; ID 264 to 265, slide No. 2140 to 2141, 3039, 3217 to 3218; ELTE.

Description

Short description of fixed specimens:

Measurements. Body length 11–16 mm, segment number 55–66, 650–800 μm wide at clitellum.

Chaetae. Chaetal formula: 3,2–2:3(2)–2. Preclitellar chaetae 60–85 μm × 7 μm ventrally, 55–58 μm × 6 μm laterally, postclitellar chaetae 75–85 μm × 6 μm ventrally, and 58–75 μm × 6 μm laterally.

Dorsal vessel. From XIII–XIV.

Sperm sacs. Large sperm sacs, located in X–XI.

Sperm funnel. 376 μm long, about 3 × as long as wide, fixed. Sperm duct about the same wide in all length (20–25 μm wide).

Male copulatory organs. Male glands multiple: one larger rounded primary bulb (diameter 75–85 μm) and numerous smaller glands.

Spermathecae. Ectal duct of spermatheca 62–90 μm long with large glands around orifice of duct. Ampulla spherical (diameter 120–140 μm) with one diverticulum (about 270 μm long), or 2–3 smaller diverticula (80–110 μm long). Additional specimens would be required for accurate description.

Distribution and habitat

Kongsfjorden, Svalbard, under a bird cliff ‘compost’ of bird excrements, mosses, vascular plants and nest material.

Enchytraeus sp.3 from Kerguelen Islands

Material examined

KERGUELEN ISLANDS • 5 specs; Ile Guillou Island; ID 260 to 261, slide No. 3035 to 3037; ELTE.

Description

Based on the few specimens in imperfect condition, *Echytraeus* sp.3 from Kerguelen Islands is very similar morphologically to *E. albidus* s. str.

Measurements. Body length 10–13 mm, segment number 44–54, 610–660 μm wide at clitellum, fixed.

Chaetae. Chaetal formula: 3–2,3:3,4–2,3. 87–95 μm × 8 μm in ventral bundles, 77–80 μm × 7.5 μm in lateral bundles preclitellarly and 77–80 μm × 7 μm in ventral bundles and 62–70 μm × 5 μm in lateral bundles posteriorly.

Dorsal vessel. from XIII–XIV.

Coelomocytes. 31–42 μm long.

Sperm sacs. Large sperm sacs, located in X–XI.

Sperm funnel. 375–550 μm long, about 4 × as long as wide, fixed.

Spermatozoa. About 60 μm long, heads 18 μm. Sperm duct about same wide in all length (23–30 μm wide).

Male copulatory organs. Male glands multiple: one larger rounded primary bulb (80–100 μm, fixed) and numerous smaller glands.

Spermathecae. Ectal duct of spermatheca with glands around duct, not only at the orifice. Ampulla with one diverticulum (about 210 μm long, fixed).

Distribution and habitat

Guillou Island, Kerguelen Islands, under a small clump of *Poa kerguelensis*.

Results of molecular analysis

Results of molecular analysis corroborated that *E. adrianensis* sp. nov., *E. andrasi* sp. nov. and *E. andrasiformis* sp. nov. are new, distinct species, since the sequences obtained from the examined individuals clearly separated in the phylogenetic trees (Figs 10–12). Our study also provided new reference sequences for *E. albidus* s. str., *E. irregularis*, *E. krumbachi*, and it provided sequences for further unnamed taxa within the *E. albidus* group (*E.* sp.2 and *E.* sp.3). *Enchytraeus andrasi* sp. nov. and *E. andrasiformis* formed distinct lineages, they were placed outside the clade of the *E. albidus* complex in the phylogenetic trees. The p-distances between the COI sequences of *E. andrasi* and *E. andrasiformis* are 16.8–17.6%, the H3 distances between them are 3%. The COI distances between *E. andrasi* and the members of *E. albidus* complex (including *E. adrianensis*) are 15.9–20.6%, the H3 distances between them are 5.4–8.5%. The intraspecific COI distances between specimens of *E. andrasi* are 0–1.8%. There are no intraspecific differences between the H3 sequences of *E. andrasi* individuals. The COI distances between *E. andrasiformis* and the species of *E. albidus* complex (including *E. adrianensis* sp. nov.) are 15.6–20.3%, the H3 distances between them are 5.2–8.1%. *Enchytraeus adrianensis* and additional species missing from the study of Erséus *et al.* (2019), namely *E. irregularis*, *E.* sp.2 and *E.* sp.3 were placed inside the clade of the *E. albidus* complex. The COI distances between *E. adrianensis* and members of *E. albidus* complex are 12.8–17.8%, the H3 distances between them are 0.4–5.5%. There are no intraspecific differences between the COI and between the H3 sequences of specimens of *E. adrianensis*. *Enchytraeus* sp.2 and *E.* sp.3 formed one group on the gene trees. It is worth noting that the COI distance between *E.* sp.2 and *E.* sp.3 is very small (0.2%), while the H3 distance between them is bigger (2.5%), and comparable to interspecific differences in the rest of the H3 gene tree (Fig. 11). *Enchytraeus adrianensis* appeared as the sister group of *E. krumbachi* in the COI and H3 gene trees, and *E. irregularis* appeared as the sister group of *E.* sp.2 / sp.3 clade in both of the gene trees (Figs 10–11). The COI distances between *E. adrianensis* and *E. krumbachi* are 12.9–13.4%, the H3 distances between them are low, 0.4–1.6%. The COI distances between *E. irregularis* and *E.* sp.2 / sp.3 clade are 12.2–12.9%, the H3 distances between them are 2.1–3.8%. According to the molecular analysis, our *E. krumbachi* individuals and *E.* cf. *krumbachi* CE1684 and CE1689 specimens belong to the same species. The intraspecific COI distances between our *E. krumbachi* and *E.* cf. *krumbachi* individuals are 0.7–3%, the intraspecific H3 distances between them are 0–0.8%. On the species tree (Fig. 12), the *E. albidus* complex formed a distinct clade with maximum posterior probability support and contains *E. adrianensis*, *E. irregularis* and *E.* sp.2 / sp.3, as in the gene trees. *E. adrianensis* sp. nov. appeared as the sister group of *E. krumbachi, E.* sp.2 / sp.3 appeared as the sister group of *E. irregularis*. *Enchytraeus andrasi* and *E. andrasiformis* were placed outside the *E. albidus* complex and they appeared there as sister groups of each other. *E. andrasi* and *E. andrasiformis* clustered with *E. norvegicus* Abrahamsen, 1969 on the species tree (Fig. 12) but with only low posterior probability support, and the latter species differs from the new species in many traits.

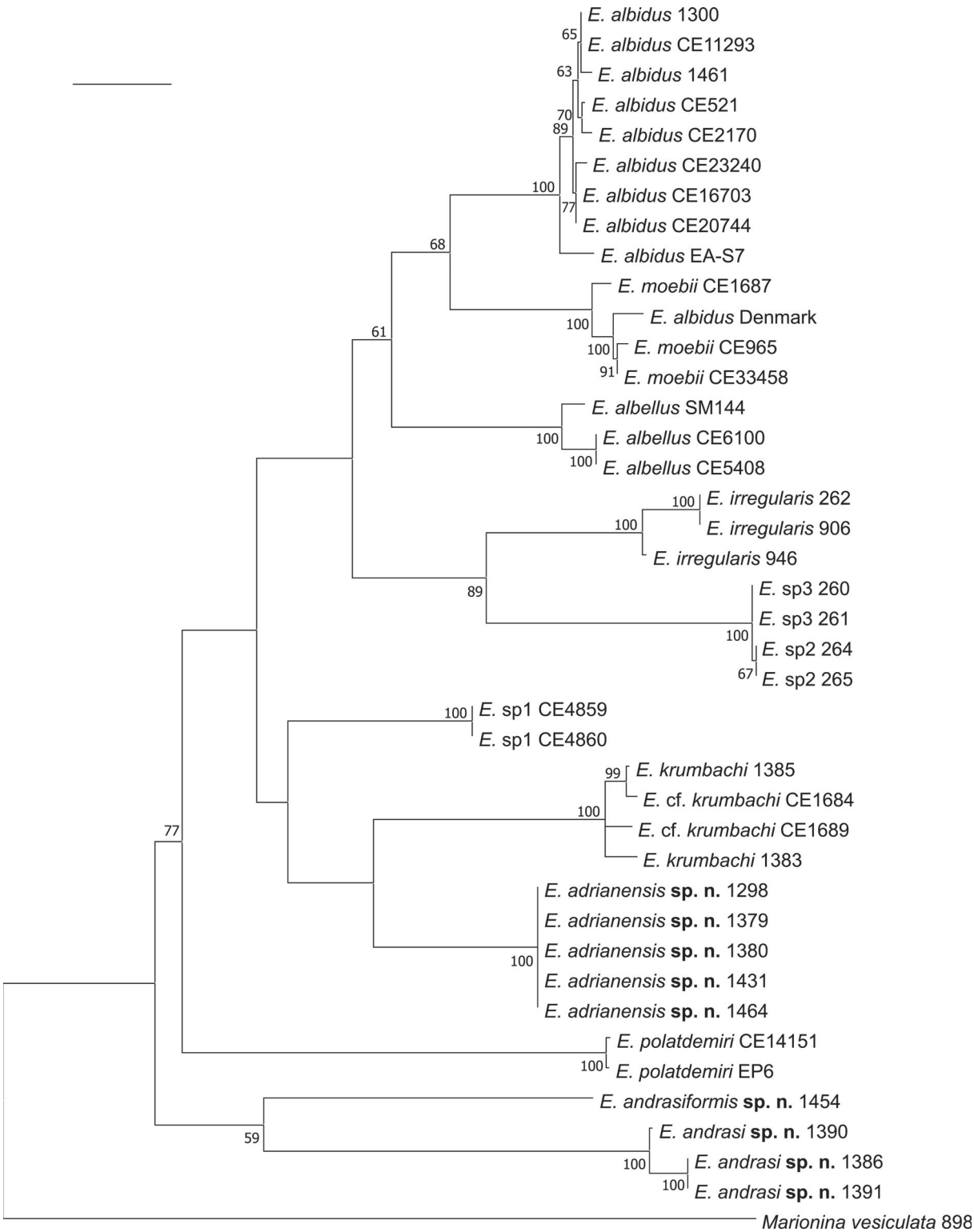

Fig. 10. Maximum likelihood (ML) tree of the COI gene for specimens of the *Enchytraeus albidus* species complex, based on 568 nucleotide positions using the General Time Reversible substitution model. Bootstrap values greater than 50 are shown at the nodes. Accession codes of sequences with collection information are given in Table 1. Scale bar: 0.05 substitutions per nucleotide.

Discussion

Comparing our results with the results of morphological and molecular analysis of the *E. albidus* complex in Erséus *et al.* (2019) and in Arslan *et al.* (2018), we can state that this species complex includes many species and we can assume the existence of additional new species in the *E. albidus* complex. Most of the known species are morphologically very similar to each other, but yet some morphological differences are ascertainable (Table 2), and genetic data have supported their delimitation as separate species. For instance, the results of our molecular investigation supported the taxonomic status of the three new species of *Enchytraeus* described here. These genetic differences can be explained by the existence of

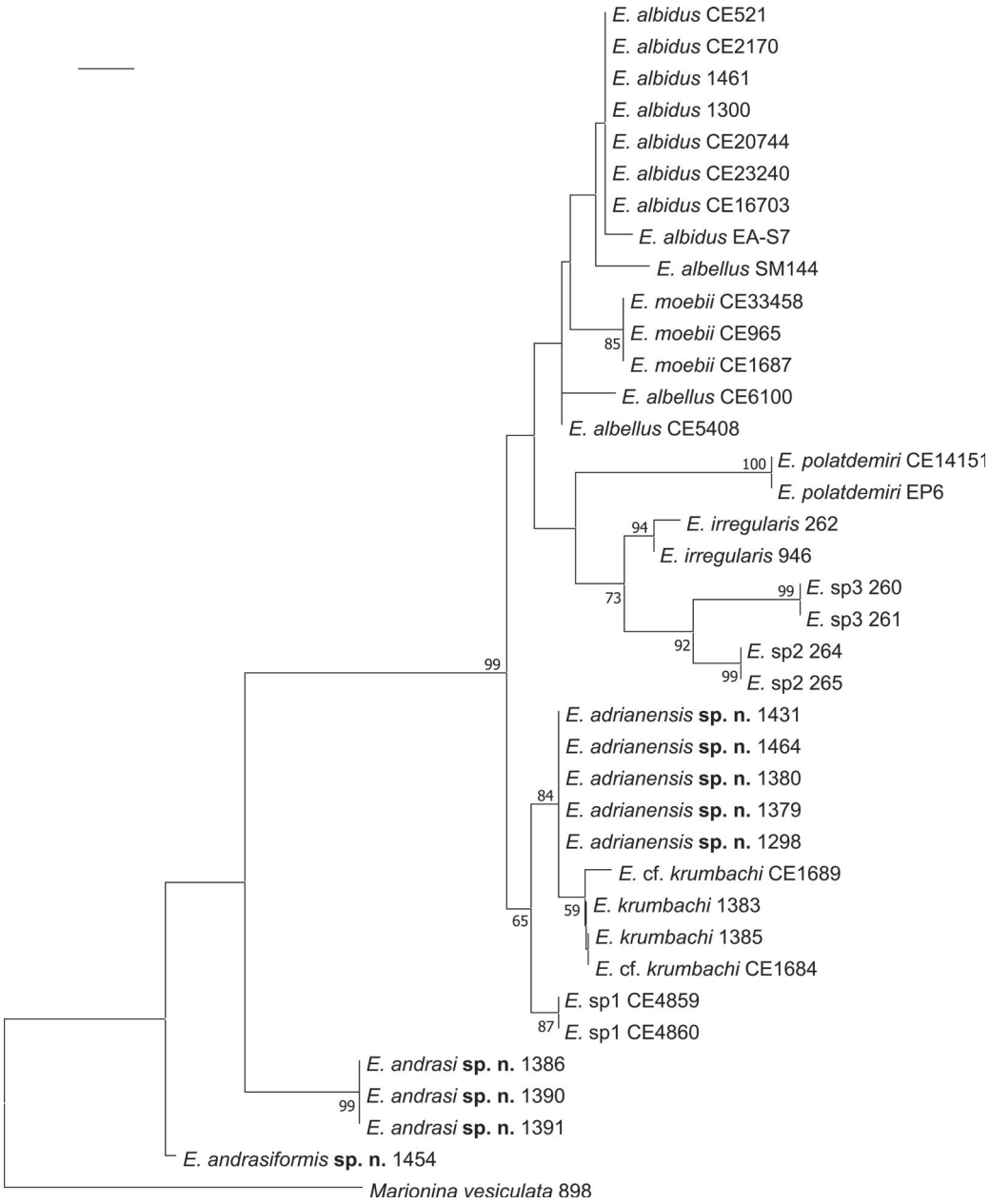

Fig. 11. Maximum likelihood (ML) tree of the H3 gene for specimens of the *Enchytraeus albidus* species complex, based on 225 nucleotide positions using the Kimura 2-parameter substitution model. Bootstrap values greater than 50 are shown at the nodes. Accession codes of sequences with collection information are given in Table 1. Scale bar: 0.01 substitutions per nucleotide.

an ancestral species with high genetic variability. As recent species live mostly in the decaying seaweed on seashores and widespread throughout the world from Arctic Svalbard in the north to Subantarctic Kerguelen Islands in the south, they possibly evolved into different species under the influence of distinct climatic and ecological pressures. Other possible causes of species radiation are parthenogenesis or self-fertilizing reproduction among enchytraeids (Christensen 1960, 1961; Dózsa-Farkas 1995), but this has not been proven yet in the species of the *E. albidus* group. *Enchytraeus andrasi* sp. nov. and *E. andrasiformis* sp. nov. were placed outside the clade of the *E. albidus* complex in the gene trees and in the species tree. It is possible that these two species evolved from the hypothetical ancestral species into new species earlier than the other members of the *E. albidus* complex, or perhaps, despite the morphological similarities, *E. andrasi* and *E. andrasiformis* are not members of the *E. albidus* complex genetically and they are distinct lineages. According to their positions in the species tree, they are closely related to each other, and their insertion within the non-albidus *Enchytraeus* group seems to support the latter hypothesis. Further research is required to clarify the exact phylogenetic position of *E. andrasi* and *E. andrasiformis*, and their relationship with the *E. albidus* group. Based on its position in the phylogenetic trees, *E. adrianensis* sp. nov. is a member of the *E. albidus* complex and the closest relative of *E. krumbachi*. The COI distances between *E. adrianensis* and *E. krumbachi* are greater than 10% (12.9–13.4%). In clitellates, if two lineages differ with more than 10% genetic distance (in case of COI gene), they are assumed to belong to different species (Rougerie *et al.* 2009). But it has to be noted that the H3 distances between *E. adrianensis* and *E. krumbachi* are low (0.4–1.6%), therefore *E. adrianensis* is unresolved from *E. krumbachi* on the H3 tree. It can be mentioned, that there are similarly low distance values in case of other species of the *E. albidus* group. For example, according to our results, the COI distances between *E. albellus* and *E. albidus* s. str. are 11.1–12.7%, the H3 distances between them are 0.4–2%. We did not find *E. krumbachi* in the Adriatic samples and did not find *E. adrianensis* in the Italian samples. Furthermore, they are closely related species based on the molecular results, so it is possible that *E. adrianensis* evolved from a local population of *E. krumbachi*, or vice versa, or from a common ancestor. Results of the phylogenetic analysis revealed that the Italian *E. krumbachi* specimens identified by us and *E.* cf. *krumbachi* CE1684 and CE1689 individuals (Erséus *et al.* 2019) from Spain belong to the same species. The genetic distances also supported this result. In the case of *E. krumbachi*, it seems that our specimens agree better with the morphological description

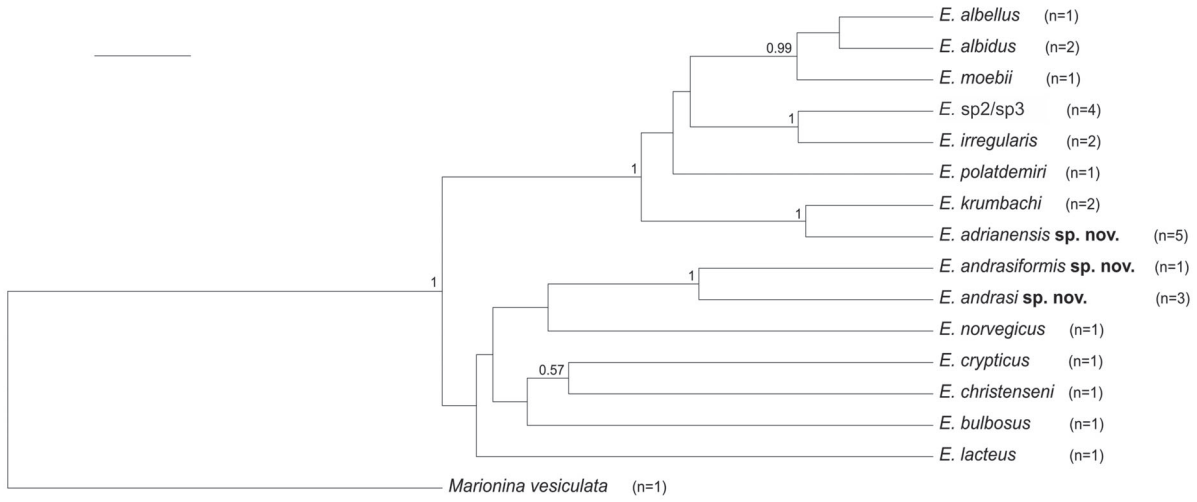

Fig. 12. *Enchytraeus* Henle, 1837 species tree, based on COI, H3 and 16S rRNA gene (Bayes analysis, *BEAST). Posterior probabilities greater than 0.5 are shown at the nodes. Accession codes of sequences with collection information are given in Table 1. Abbreviation: n = number of included specimens for each species. Scale bar = 0.07 substitutions per nucleotide.

of Čejka (1913). Despite the differences given by Erséus *et al.* (2019) in chaetal number and the small chamber of spermathecal ampulla, we think that these differences denote only intraspecific variation, especially if we take into account the different geographical locality. The *E.* sp.2 / sp.3 clade was included to the *E. albidus* complex in this study, and the studied specimens were separated from all the other studied species in the phylogenetic trees. *E.* sp.2 individuals from Svalbard and *E.* sp.3 specimens from Kerguelen Islands are the same species according to the COI gene tree, but they show greater genetic distance between H3 sequences. Since COI evolves faster than H3 gene, we expected that the distance between COI sequences would be larger. Unfortunately, specimens of *E.* sp.2 and *E.* sp.3 were old material, therefore only a short morphological description is provided in this paper, but all these results supported that it is probably a new species and suggest the existence of further new species in the *E. albidus* complex. New and fresh material is needed for a detailed morphological description and for further molecular analysis of *E.* sp.2 and *E.* sp.3.

It is worth mentioning, that the phenomenon of 'surplus chaetae' is common in almost all species. The frequent existence of this suggests, either there is a frequent change of chaetae in these species, or older chaetae remain for a longer period of time. Similarly to *E. albidus*, *E. adrianensis* sp. nov. fed with oat can be cultured easily. As an interesting observation, individuals fed with abundant food often became bigger (in body length and segment number) than the native specimens collected originally from seashore.

To summarize the current status of the genus *Enchytraeus*, the type genus of the family Enchytraeidae, in this paper we described three species new to science (*E. adrianensis* sp. nov., *E. andrasi* sp. nov., *E. andrasiformis* sp. nov.) and added essential reference DNA sequences for other species within this genus (*E. irregularis*). As a result, the number of valid species of *Enchytraeus* is 55 now: 21 of them are morphologically described with available DNA reference data (*E. adrianensis*, *E. andrasi*, *E. andrasiformis*, *E. albidus* s. str.*, E. albellus, E. bigeminus* Nielsen & Christensen, 1963*, E. buchholzi* Vejdovský, 1879*, E. bulbosus* Nielsen & Christenesen, 1963*, E. christenseni* Dózsa-Farkas, 1992*, E. coronatus* Nielsen & Christensen, 1959*, E. crypticus* Westheide & Graefe, 1992*, E. demutatus* Schmelz, Klinth, Chalkia, Anastasiadou & Vavoulidou, 2019*, E. dichaetus* Schmelz & Collado, 2010*, E. doerjesi* Westheide & Graefe, 1992*, E. irregularis, E. japonensis* Nakamura, 1993*, E. krumbachi, E. lacteus* Nielsen & Christensen, 1961*, E. moebii, E. norvegicus, E. polatdemiri*). 34 species of *Enchytraeus* are described solely on morphological features without DNA reference sequences (checklist of species of *Enchytraeus* in Schmelz & Collado 2012). It turned out that at least two additional species exist within this genus which was indicated with DNA-based analyses but further morphological studies are needed for species descriptions (*E*. sp.1, sp.2 and sp.3).

Acknowledgements

T. Felföldi was supported by the János Bolyai Research Scholarship of the Hungarian Academy of Sciences (grant no. BO/00837/20/8) and H. Nagy by the ÚNKP-20-4 New National Excellence Program of the Ministry for Innovation and Technology from the source of the National Research, Development and Innovation Fund, Hungary (grant no. ÚNKP-20-4-I-ELTE-281). The authors are thankful to András and Kinga Dózsa-Farkas, Dr Júlia Török, Dr Tone Birkemoe, Dr Yves Frenot, Dr Yong Hong and Dr Csaba Csuzdi for collecting worms and substrate samples and to György Makranczy for English proofreading.

References

Arslan N., Timm T., Rojo V., Vizcaíno A. & Schmelz R.M. 2018. A new species of *Enchytraeus* (Enchytraeidae, Oligochaeta) from the profundal of Lake Van, the world's largest soda lake (Turkey, East Anatolia). *Zootaxa* 4382 (2): 367–380. https://doi.org/10.11646/zootaxa.4382.2.8

Bely A.E. & Wray G.A. 2004. Molecular phylogeny of naidid worms (Annelida: Clitellata) based on cytochrome oxidase I. *Molecular Phylogenetics and Evolution* 30: 50–63. https://doi.org/10.1016/S1055-7903(03)00180-5

Birkemoe T. & Dózsa-Farkas K. 1994. New records of Enchytraeidae (Oligochaeta) from Spitsbergen, Svalbard. *Fauna Norvegica Series A* 15: 35–44.

Bouckaert R., Heled J., Kühnert D., Vaughan T., Wu C-H., Xie D., Suchard M.A., Rambaut A. & Drummond A.J. 2014. BEAST 2: A Software Platform for Bayesian Evolutionary Analysis. *PLoS Computational Biology* 10: e1003537. https://doi.org/10.1371/journal.pcbi.1003537

Čejka B. 1913. *Litorea krumbachi* n. spec. n. gen. Ein Beitrag zur Systematik der Enchytraeiden. *Zoologischer Anzeiger* 17: 145–151.

Christensen B. 1960. A comparative cytological investigation of the reproductive cycle of an amphimictic diploid and a parthenogenetic triploid form of *Lumbricillus lineatus* (O.F.M.) (Oligochaeta, Enchytraeidae). *Chromosoma* 11: 365–379. https://doi.org/10.1007/BF00328661

Christensen B. 1961. Studies on cyto-taxonomy and reproduction in the Enchytraeidae with notes on parthenogenesis and polyploidy in the animal kingdom. *Hereditas* 47: 387–450.

Christensen B. & Glenner H. 2010. Molecular phylogeny of Enchytraeidae (Oligochaeta) indicates separate invasions of the terrestrial environment. *Journal of Zoological Systematics and Evolutionary Research* 48: 208–212. https://doi.org/10.1111/j.1439-0469.2009.00558.x

Coates K. & Ellis D.V. 1981. Taxonomy and distribution of marine Enchytraeidae (Oligochaeta) in British Columbia. *Canadian Journal of Zoology* 59: 2129–2150.

Colgan D.J., McLauchlan A.A., Wilson G.D.F., Livingston S.P., Edgecombe G.D., Macaranas J., Cassis G. & Gray M.R. 1998. Histone H3 and U2 snRNA DNA sequences and arthropod molecular evolution. *Australian Journal of Zoology* 46: 419–437. https://doi.org/10.1071/ZO98048

Collado R., Schmelz R., Moser T. & Römbke J. 1999. Enchytraeid Reproduction Test (ERT): Sublethal responses of two *Enchytraeus* species (Oligochaeta) to toxic chemicals. *Pedobiologia* 43: 625–629.

CorelDRAW Graphic Suite 2021. Available from https://www.coreldraw.com/de/pages/coreldraw-2021/ [accessed 24 Apr. 2023].

Dózsa-Farkas K. 1995. Self-fertilisation: An adaptive strategy in widespread enchytraeids. *European Journal of Soil Biology* 31 (4): 207–215.

Dózsa-Farkas K., Felföldi T. & Hong Y. 2015. New enchytraeid species (Enchytraeidae, Oligochaeta) from Korea. *Zootaxa* 4006 (1): 171–197. https://doi.org/10.11646/zootaxa.4006.1.9

Dózsa-Farkas K. 2019. Enchytraeids of Hungary (Annelida: Clitellata: Enchytraeidae). *Pedozoologica Hungarica* 7. Eötvös University Press, Budapest.

d'Udekem J. 1855. Nouvelles classification des Annélides sétigères abranches. *Bulletins de l'Académie royale des sciences, des lettres et des beaux-arts de Belgique* 22 (2): 533–557.

Eisen G. 1904. Enchytraeidae of the west Coast of North America. *Harriman Alaska Series*. New York 12: 1–126.

Erséus C. & Gustafsson D. 2009. Cryptic speciation in clitellate model organisms. *In: Annelids in Modern Biology*. John Wiley & Sons, Hoboken.

Erséus C., Rota E., Matamoros L. & De Wit P. 2010. Molecular phylogeny of Enchytraeidae (Annelida, Clitellata). *Molecular Phylogenetics and Evolution* 57 (2): 849–858. https://doi.org/10.1016/j.ympev.2010.07.005

Erséus C., Klinth M.J., Rota E., Wit P.D., Gustafsson D.R. & Martinsson S. 2019. The popular model annelid *Enchytraeus albidus* is only one species in a complex of seashore white worms (Clitellata, Enchytraeidae). *Organisms Diversity & Evolution* 19: 105–133. https://doi.org/10.1007/s13127-019-00402-6

Folmer O., Black M., Hoeh W., Lutz R. & Vrijenhoek R. 1994. DNA primers for amplification of mitochondrial cytochrome c oxidase subunit I from diverse metazoan invertebrates. *Molecular Marine Biology and Biotechnology* 3: 294–299.

Heled J. & Drummond A.J. 2010. Bayesian inference of species trees from multilocus data. *Molecular Biology and Evolution* 27: 570–580. https://doi.org/10.1093/molbev/msp274

Henle F.G.J. 1837. Ueber *Enchytraeus*, eine neue Anneliden-Gattung. *Archiv für Anatomie, Physiologie und Wissenschaftliche Medicin* 74–90.

Hong Y. & Dózsa-Farkas K. 2018. New description of enchytraeid species (Clitellata: Enchytraeidae) from Korea. *Journal of Species Research* 7: 80–91. https://doi.org/10.12651/JSR.2018.7.1.080

INKSCAPE 1.2.2 – Draw freely. Available from https://inkscape.org [accessed 24 Apr. 2023].

Kane R.A. & Rollinson D. 1994. Repetitive sequences in the ribosomal DNA internal transcribed spacer of *Schistosoma haematobium*, *Schistosoma intercalatum* and *Schistosoma mattheii*. *Molecular and Biochemical Parasitology* 63: 153–156. https://doi.org/10.1016/0166-6851(94)90018-3

Kasprzak K. 1984. The previous and contemporary conceptions on phylogeny and systematic classifications of Oligochaeta Annelida. *Annales zoologici, Warszawa* 38 (9): 205–223.

Kumar S., Stecher G. & Tamura K. 2016. MEGA7: Molecular Evolutionary Genetics Analysis version 7.0 for bigger datasets. *Molecular Biology and Evolution* 33: 1870–1874. https://doi.org/10.1093/molbev/msw054

Martinsson S. & Erséus C. 2018. Cryptic diversity in supposedly species-poor genera of Enchytraeidae (Annelida: Clitellata). *Zoological Journal of the Linnean Society* 183: 749–762. https://doi.org/10.1093/zoolinnean/zlx084

Matamoros L., Rota E. & Erséus C. 2012. Cryptic diversity among the achaetous *Marionina* (Annelida, Clitellata, Enchytraeidae). *Systematics and Biodiversity* 10 (4): 509–525. https://doi.org/10.1080/14772000.2012.723640

Michaelsen W. 1885. Vorlaufige Mitteilungen über *Archenchytraeus Möbii* n. sp. *Zoologischer Anzeiger* 8: 237–239.

Michaelsen W. 1886. *Untersuchungen über Enchytraeus Möbii Mich. und andere Enchytraeiden*. Lipsius & Tischer, Kiel.

Michaelsen W. 1919. Über die Beziehungen der Hirudineen zu den Oligochäten. *Mitteilungen aus dem Hamburgischen zoologischen Museum und Institut* 36: 131–153.

Michaelsen W. 1926. Zur Kenntnis einheimischer und ausländischer Oligochäten. *Zoologische Jahrbücher Abteilung für Systematik, Geographie und Biologie der Tiere* 51: 255–328.

Nielsen C.O. & Christensen B. 1959. The Enchytraeidae. Critical revision and taxonomy of European species (studies on Enchytraeidae VII). *Natura Jutlandica* 8–9: 1–160.

Nielsen C.O. & Christensen B. 1961. The Enchytraeidae. Critical revision and taxonomy of European species. Supplement 1. *Natura Jutlandica* 10: 1–23.

O'Connor F.B. 1962. The extraction of Enchytraeidae from soil. *In*: Murphy P.W. (ed.) *Progress in Soil Zoology*: 279–285. Butterworths Publishers, London.

Rambaut A. 2018. FigTree version 1.4.4. Computer program and documentation distributed by the author. Available from http://tree.bio.ed.ac.uk/software/figtree/ [accessed 25 Apr 2023].

Rambaut A., Drummond A.J., Xie D., Baele G. & Suchard M.A. 2018. Posterior summarisation in Bayesian phylogenetics using Tracer 1.7. *Systematic Biology* syy032. https://doi.org/10.1093/sysbio/syy032

Rougerie R., Decaëns T., Deharveng L., Porco D., James S.W., Chang C.-H., Richard B., Potapov M., Suhardjono Y. & Hebert, P.D.N. 2009. DNA barcodes for soil animal taxonomy. *Pesquisa Agropecuaria Brasileira* 44: 789–802. https://doi.org/10.1590/S0100-204X2009000800002

Römbke J. 1989. *Enchytraeus albidus* (Enchytraeidae, Oligochaeta) as a test organism in terrestrial laboratory systems. *Archives of Toxicology,* Suppl. 13: 402–405. https://doi.org/10.1007/978-3-642-74117-3_79

Schmelz R.M. & Collado R. 2010. A guide to European terrestrial and freshwater species of Enchytraeidae (Oligochaeta). *Soil Organisms* 82: 1–176.

Schmelz R.M. & Collado R. 2012. An updated checklist of currently accepted species of Enchytraeidae (Oligochaeta, Annelida). *Newsletter on Enchytraeidae* 12: 67–87.

Sjölin E., Erséus C. & Källersjo M. 2005. Phylogeny of Tubificidae (Annelida, Clitellata) based on mitochondrial and nuclear sequence data. *Molecular Phylogenetics and Evolution* 35: 431–441. https://doi.org/10.1016/j.ympev.2004.12.018

von Bülow T. 1957. Systematisch-autökologische Studien an eulitoralen Oligochaeten der Kimbrischen Halbinsel. *Kieler Meeresforschungen* 13: 96–116.

White T.J., Bruns T., Lee S. & Taylor J. 1990. Amplification and direct sequencing of fungal ribosomal RNA genes for phylogenetics. *In*: Innis M.A., Gelfand D.H., Sninsky J.J. & White T.J. (eds) *PCR Protocols: A Guide to Methods and Applications*: 315–322. Academy Press, San Diego.

Manuscript received: 24 March 2022
Manuscript accepted: 12 January 2023
Published on: 26 May 2023
Topic editor: Tony Robillard
Desk editor: Eva-Maria Levermann